Exploring Methods for the Characterization of Viral RNA-protein Complexes

by

Zlatko Lejic

A thesis
presented to the University of Waterloo
in fulfillment of the
thesis requirement for the degree of
Master of Science
in
Chemistry

Waterloo, Ontario, Canada, 2009

AUTHOR'S DECLARATION

I hereby declare that I am the sole author of this thesis. This is a true copy of the thesis, including any required final revisions, as accepted by my examiners.

I understand that my thesis may be made electronically available to the public.

ABSTRACT

Flock House virus (FHV) is a (+) ssRNA virus that belongs to the *Nodaviridae* family. The viral genome is composed of two viral RNA's: RNA 1 and RNA 2. Deletion and mutation studies in the N- and C-terminus of protein alpha have identified protein regions required for the packaging of FHV viral RNAs. Residues 2-31 on the N-terminus have been attributed with RNA2 recognition, while residues at positions 32-50 were required for the packaging of RNA1. The C-terminus is needed for packaging of both viral RNAs. The identified protein regions involved in packaging viral RNAs bind random cellular RNA with high affinity and standard methods of identifying RNA-protein interactions such as gel shift mobility assays will be unable to discriminate between specific and unspecific binding. Due to the difficulty in differentiating between specific and unspecific binding a new method for studying RNA-protein interactions was developed using a surface based detection approach. The surface based system monitors real-time binding, whereby specific and unspecific RNA-protein interactions will be distinguished through comparison of relative association rates for each binding interaction. A well studied RNA-protein interaction, the HIV-1 Rev-RRE, was used to develop the methodology for the surface based system.

Human immunodeficiency virus type 1 (HIV-1) encodes a regulatory protein Rev that binds to HIV-1 mRNA of the Rev responsive element (RRE). Rev-RRE interaction regulates viral gene expression by controlling the export of spliced and unspliced mRNAs into the cytoplasm. The high-affinity and specificity of the Rev-RRE binding has been well characterized and was used as a model system to gauge the sensitivity of the surface based detection system, which can be further used to characterize various RNA-protein interactions.

The surface based system uses diffractive optics to detect real time binding of molecules to receptors that are immobilized on a flat sensor surface. An avidin coated sensor surface was applied to couple the small biotinylated Rev peptide to the surface followed by binding its

complementary RRE RNA. The binding interactions of the 30 nucleotide RRE to the immobilized 23 residue Rev peptide were successfully monitored using the avidin sensor. The Rev-RRE interaction was heavily influenced by the immobilization technique and steric hindrance at the sensor surface.

ACKNOWLEDGEMENTS

I would like to acknowledge those individuals who contributed their time, effort and support during the development and completion of my MSc. degree in Chemistry at the University of Waterloo.

First and foremost, I would like to thank my supervisor, Dr. Thorsten Dieckmann, who has given me the chance to pursue an area of research I was curious about. He challenged me to reach my fullest potential, while at the same time providing guidance and support during the course of this journey.

To the members of my committee, Dr. Guy Guillemette and Dr. Michael Palmer, I am thankful for their time, support and feedback.

I would like to express my gratitude to those who helped me along the way and have made this thesis project possible. To my lab members who generously shared their knowledge and gave invaluable feedback; particularly, Allen Chu for his assistance with various aspects of the research, and Jason DaCosta for the long hours he contributed to mass spectroscopy.

A special thank you goes to Dr. Zhengding Su for his advice, guidance and vast knowledge with the peptide purification.

I would also like to thank all the friends I have made over the years, both in and outside the department. Your friendship was an immense motivator that has aided and encouraged me during my studies. Thank you for all the coffee runs, laughs shared, and memorable times spent together.

Finally, to my parents and sister: thank you for your unconditional love, encouragement and belief in me throughout all my endeavours.

.

CONTENTS

LIST OF TABLES

LIST OF FIGURES

Chapter 2: The Rev-RRE System

Chapter 3: Flock House virus

APPENDICES

A1.Supplementary Information

A2. Labeling and Purification of eNOS peptide

LIST OF ABBREVIATIONS

(+) RNA	positive strand RNA
(+) ssRNA	positive single stranded RNA
AMV	Alfalfa mosaic virus
ARM	Arginine rich RNA binding motif
ATP	Adenosine triphosphate
bp	base pair
BSA	Bovine serum albumin
Bt-Rev	Biotin Rev
CPE	Cytopathic Effect
CTP	Cytosine triphosphate
DMF	Dimethylformamide
DNA	Deoxyribonucleic acid
dsRNA	double stranded RNA
Env	Envelope gene
ESI	Electrospray ionization
FHV	Flock House virus
Gag	Group specific antigen gene
GTP	Guanosine triphosphate
HIV	Human Immunodeficiency virus
IRES	Internal Ribosome Entry Site
LTR	long terminal repeats
LUCA	Last Universal Common Ancestor
^{m7}G	7-methylguanosine cap
mRNA	messenger RNA
MS	mass spectrophotometry
Nef	Negative Factor
NES	Nuclear Export Signal
nf. Water	nuclease free Water
NLS	Nuclear Localization Signal
NPC	Nuclear Pore Complex
nt	nucleotide
PAGE	polyacrylamide gel electrophoresis
Pol	Polymerase gene
Pvr	Poliovirus receptor
Rd-RP	RNA dependant- RNA polymerase
Rev	Regulator of virion
RISC	RNA-induced silencing complex
RNA	Ribonucleic acid
RNAi	RNA interference

RP-HPLC	Reverse Phase- High performance liquid chromatography
RRE	Rev Responsive Element
SARS	Severe acute respiratory syndrome
siRNA	Small interfering RNAs
T	Triangulation number
TAR	Transactivation Response region
tRNA	transfer RNA
UTP	Uridine triphosphate
UTR	untranslated region
Vif	Viral infectivity factor
VP	Viral protein
Vpr	Viral protein R
Vpu	Viral protein U

Chapter 1: Introduction

1.1 Viral Evolution

Viruses are small infectious particles that act as intracellular parasites. They require an appropriate host for the production of new progeny virions. The evolution of viruses and the question of their origin has been a topic of debate for some time; viruses leave few remains and traces of their former progenitors during the course of their lifetime, and so their origin and evolution are difficult to track (*1*). Two main views exist on the emergence of viruses, the first one stating that viruses are cellular elements that have obtained the ability to self-replicate and self-assemble. The second view suggests that viruses evolved in the prebiotic world prior to cellular organisms and are left over evidence of the hypothetical RNA world (*1*). Conclusive evidence supporting either theory does not exist, although studies of viral genomes and structure are providing insight as to which theory may fit best.

The notion that viruses originated from cellular elements can be further broken down into two separate theories: the regressive and the cellular origin theories. The regressive theory suggests that viruses have devolved from intracellular parasites that have lost the ability to govern their own metabolic functions and only retained genes required to support their parasitic nature (*1, 2*). The regressive evolution theory is rejected predominantly for two reasons: because parasites derived from the three domains (Bacteria, Eukaryotes, Archaea) of life currently known, are still capable of producing their own proteins and energy and because no known intermediate states exist between cells and viruses. It has been proposed that the regressive theory could be applied to early RNA cells due to their simplicity compared to present-day cells. Early RNA cells living endosymbiotically in other RNA cells could have adopted a parasitic nature and lost key pathways for protein and energy production; the loss of specific metabolic pathways has been observed in existing parasites (*2*). The cellular origin theory explores the possibility of viruses arising from cellular genetic

fragments that have broken away from their normal function and established a parasitic lifestyle (*1, 2*). It has been suggested that the cellular origin theory would be easier to defend if taken in the context of a pre-Last Universal Common Ancestor (LUCA) time. LUCA is considered to be the last link from which the three cellular domains have evolved. Early RNA cells in the pre-LUCA period were believed to contain segmented genomes, still observed in some RNA viruses, which would be more susceptible to becoming autonomous (*2*).

The coevolution of viruses along with cells in a prebiotic world with the assistance of self-replicating molecules is an integral part of the current view on viral evolution in a hypothetical RNA world. The RNA world hypothesis suggests that RNA was present before DNA and proteins and was the first chemical system capable of supporting life. DNA and proteins evolved later and retained close interaction with RNA.(*3*) Early viruses employed RNA to store genetic information and used this primordial soup as a host system. Remnants of the RNA world can be observed through the study of viral structures. Eukaryotic viruses such as the Polio virus contain 5' untranslated regions (UTR) that have tRNA-like structures used in regulating translation; similar structures are seen at the 3' UTR in plant virus genomes (*3*). Internal ribosome entry sites (IRES) are used by both viruses and cells that come from various organisms differing in complexity. IRES are approximately 180 nucleotides long and form triple pseudoknot RNA structures involved in translation initiation. IRES maintain high efficiency and take the place of proteins that act as translation initiation factors (*3*). There are no methods that can test any of the views on viral evolution, although some insight can be gained by studying new emerging strains of viruses whose lineage can be directly traced, such as new strains of the Influenza virus and emerging coronaviruses (SARS-CoV).

Viruses have been in existence for some considerable time as they have diverse hosts ranging from plants to insects to higher animals. The rapid evolution of viruses is attributed to the rate at which viral genomes acquire mutations (0.1-1% per year), leading to many divergent

classes of viruses (*4*). RNA genomes have a higher mutation rate than DNA genomes; during replication misinsertion errors have been estimated to be in the range of 10^{-3} to 10^{-5} substitutions per nucleotide per round of copying. The higher mutation rates in RNA viral genomes have been attributed to reverse transcriptase's and RNA polymerase's lack of proofreading domains (*5*). The classical classification system for new emerging viruses used primarily four delineating characteristics: the nature of the genome (DNA or RNA), the capsid symmetry, the presence of an envelope, and the dimension of the virion. Rapid development of sequencing methods has enabled complete nucleotide sequences of viral genomes to be acquired, and comparison of these genomes has led to the discovery of similarities between viruses that had previously been thought of as unrelated (*4*). Similarities discovered in viral genomes led to the grouping of viruses into superfamilies according to their genome organization. Viruses that infect different hosts (plants, animals, and insects) were found to contain many similar features in their genome belonging to different families, suggesting that these viruses evolved from a common ancestor (*4*). The *Flaviviridae* family of viruses is one example of viruses whose genome exhibits features similar to other viral families. The genomes of *Flaviviridae* viruses lack 3' end poly-(A) tails, usually observed in negative-strand RNA viruses. Instead of 3' poly-(A) tail a stable stem-and-loop structure exists, a feature seen in plant viruses. Replication and translational machinery in *Flaviviridae* viruses is organization in a similar manner as in picornaviruses (*4*). The variation in genome makeup of the *Flaviviridae* family supports the theory that viruses have evolved from a common ancestor.

RNA viruses are the most abundant group of viruses that span all kingdoms. RNA viruses are more adaptable than DNA viruses due to the plasticity of their genomes (*5*). There is a consistent need for new vaccines and antivirals to combat existing and emerging viruses; only very few viruses can be permanently controlled by either before further mutation occurs. Creating effective methods to control viruses requires an understanding of viral mechanism structures and how they function.

1.2 Research Scope

Viral RNA packaging is as yet imperfectly understood, specifically how the viral RNA is preferentially packaged over cellular RNA. Specific RNA sequences that interact with viral coat proteins during packaging have only been identified for a very few viruses by gel shift mobility experiments. Standard methods used for studying RNA-protein interactions cannot distinguish very well between specific and unspecific RNA binding. A novel method is applied to study RNA-protein interactions in positive single-stranded RNA ((+) ssRNA) viruses, using a surface based detection system. Method development with the dotLab, a surface based detection system is explored in Chapter 2 with the Rev-RRE system. Identification of RNA sequences in the Flock House virus (FHV) involved in packaging is discussed in Chapter 3.

1.3 The Axela dotLab System

The dotLab system (Axela) uses diffractive optics to detect changes on the surface of sensor chips. The configuration and function are very similar to those of surface plasmon resonance instruments. Unlike surface plasmon resonance, which uses a thin metal film excited by light to produce an oscillating wave of surface charge density (plasmon resonance), the dotLab system uses optical diffraction to detect changes on the sensor surface (*6, 7*). A bare sensor surface will not increase the diffraction signal intensity because no there is no change in the surface pattern, although upon binding a molecule of interest, the height of the sensor surface is increased and becomes patterned. These changes in turn alter the diffraction pattern due to the constructive and destructive interferences of light and produce a measurable signal recorded as diffractive index (DI) (*7*). Applications of the dotLab system are discussed in Chapter 2 and 3.

Chapter 2: The Rev-RRE System

2.1 Introduction

Human immunodeficiency virus type-1 (HIV-1) is a member of the Retroviridae family, part of the Lentivirus genus. HIV-1 contains a (+) ssRNA genome made up of two identical RNA strands joined at their 5' ends (*8*). The viral genome encodes four primary genes found among all retroviruses: gag encodes the necessary structural proteins required for capsid formation; pro, a protease, is required for processing capsid polypeptides; pol contains genetic information for reverse transcriptase, RNase H, and integrase functions; env produces envelope glycoproteins. Reverse transcriptase is an enzyme unique to the Retroviridae family and is responsible for converting the (+) ssRNA to double strand DNA (dsDNA) upon viral infection. RNase H plays an important role during reverse transcription by destroying the RNA template. The integrase activity is responsible for inserting the dsDNA into the host chromosome (*8*). HIV-1 also encodes many regulatory proteins that aid it in its lifecycle.

Regulatory proteins are translated from different mRNA splice variants and are found surrounding the env gene on the HIV-1 genome. The regulatory genes encoding regulatory proteins are tat, rev, nef, vif, vpr, and vpu (Figure 2.1) (*8, 9*). Tat protein initiates replication by binding to a 60 nucleotide stem-loop region, known as the trans-activating response region (TAR), at the 5' end of HIV-1 RNA (*9*). Negative factor (Nef) has been shown to downregulate cell surface receptor production important in eliciting a host immune response, thereby increasing HIV-1 virulence (*10, 11*). During reverse transcription, Nef was found to increase dsDNA production (*12*). Rev coordinates the transport of unspliced and partially-spliced mRNAs from the nucleus to the cytoplasm, by binding the Rev responsive element (RRE) RNA (*13*). Vif, vpr, and vpu assist the virus in viral transmission among cells, replication, and virion assembly and release (*9*). HIV-1 has been extensively studied and

many of the RNA-protein interactions have been well characterized, one being the Rev-RRE interaction.

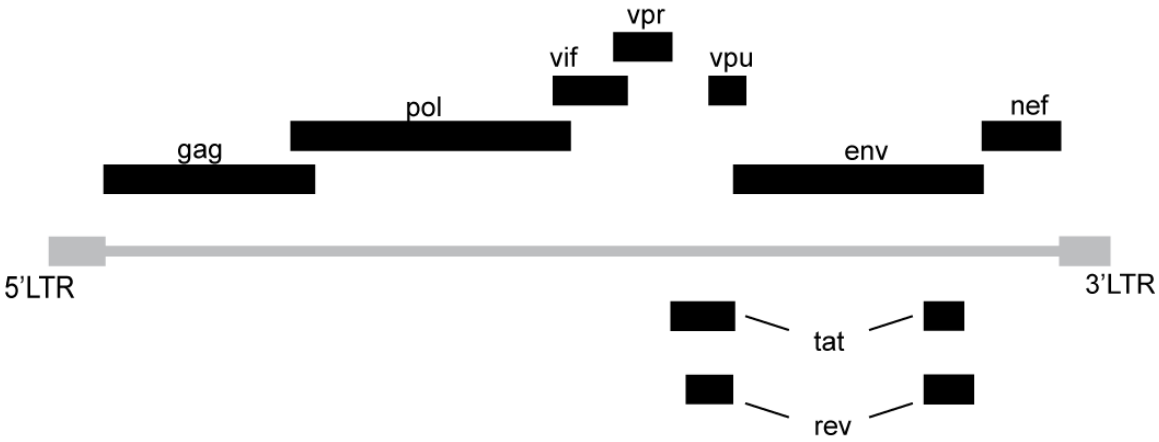

Figure 2.1- HIV-1 genome organization.

2.2 Rev-RRE Structure and Function in HIV-1

RNA-protein interactions between Rev protein and its RRE RNA counterpart function to transport unspliced mRNAs from the nucleus into the cytoplasm. Once the viral RNA has been reverse transcribed into dsDNA and integrated into a cell's chromosome by integrase, the integrated DNA is referred to as proviral DNA, and may begin transcribing. HIV-1 produces only a single RNA transcript to fill numerous roles: it serves as a template for structural proteins; its further processing allows for production of many regulatory proteins; and it is required for formation of new progeny through encapsidation. With cellular RNAs, only fully spliced mRNA containing no introns is allowed to cross the nuclear pore complex (NPC) into the cytoplasm (*14*). In contrast, HIV-1 transports full length genomic RNAs and partially spliced RNAs into the cytoplasm; HIV-1 achieves this with the Rev protein and RRE RNA interaction.

Rev is a 116 amino acid protein with two active domains and the capability to form oligomers. The N-terminal domain contains the arginine rich nuclear localization signal (NLS) enabling Rev to be transported into the nucleus through the NPC. The NLS overlaps

with the RRE binding site; the close proximity of the two signals is believed to prevent Rev from transporting the mRNA back to the nucleus. While Rev is bound to the RRE signal, the NLS signal is effectively blocked (*15, 16*). The C-terminal end has the nuclear export signal (NES), and any mutations in this region negate the transport of Rev into the cytoplasm (*17-19*). Residues 34-50 were shown to contain the essential binding site required for the Rev-RRE interaction (*20*). A 23 amino acid Rev peptide has been used to study RNA-protein interaction using NMR.

The high affinity binding site for Rev is the RRE RNA element located on the env gene (*21*). The high binding specificity of RRE towards Rev is due to its specific secondary structure. The full RRE is 351 nucleotides (nt) long, and the high affinity binding site was pinpointed to nucleotides 103-111 and 123-133 on stem region IIB and IID (*22, 23*). The binding site structure contains a 10-base internal loop surrounded by stems. Rev was shown to bind in the major groove in close proximity to the internal loop of the RRE. Upon Rev binding, a GG base pair undergoes a structural change with the ribose of one base flipping from a syn to an anti conformation (*24, 25*). The conformational change, results in a widened major groove allowing arginine and asparagine side chains to interact with specific base pairs fostering a close-fitting Rev-RRE interaction (*26*).

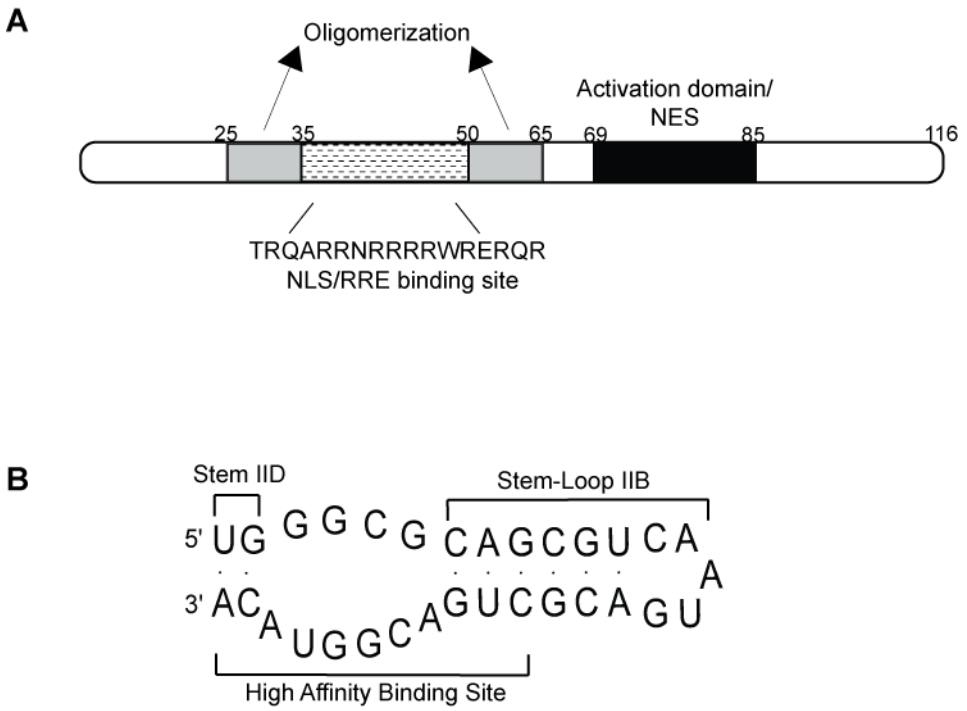

Figure 2.2- Rev-RRE high affinity binding sites.

2.3 Rev-RRE Role in Nuclear Transport

The full-length HIV-1 genome is ~9 kb, and singly spliced mRNA is ~4 kb. Both contain introns and require Rev/RRE in order to be transported into the cytoplasm for structural protein production. Fully spliced mRNAs are able to cross into the cytoplasm using a cell's export pathway and are ~2 kb each coding for Tat, Nef, and Rev (*13*). The transport of molecules from the nucleus involves NPCs, gated structures made up of many proteins called nucleoporins. Nucleoporins interact with many different transport receptor proteins to carry molecules across the nucleus membrane (*14*). Cofactors involved in the cell's transport of molecules from the nucleus have been identified as facilitating Rev in RNA transport.

Immediately after HIV-1 has infected a cell and has produced its proviral DNA, the amount of regulatory proteins is low; the majority of the transcribed viral genome is fully spliced and exported into the cytoplasm for translation. As Rev is being produced, it is transported into

the nucleus. Rev has been found to bind to importin-β, which is normally known to interact with importin-α to transport molecules into the nucleus (*16, 27*). However, the arginine-rich NLS present in Rev is very similar to the binding domain of importin-α known to interact with importin-β. It has since been suggested that Rev and importin-β interact directly in the absence of importin-α (*28, 29*). Accumulation of Rev inside the nucleus allows binding to stems IIB and IID of RRE, recruiting multiple Rev proteins to bind to a single RNA. The formation of oligomers by Rev is necessary for RNA transport to occur as it has been observed that a single Rev molecule is incapable of transporting RNA alone (*30*). The RRE-bound Rev interacts with its NES and exportin-1 for export of RNA into the cytoplasm (*31*). Exportin-1 is a member of the importin-β family of receptors and was previously known as CRM-1 (the chromosome region maintenance gene 1) (*32, 33*). The importin-β family of proteins interacts with Ran-GTP/GDP, which, through GTP hydrolysis, provides energy for the transport. Other cofactors are: eIF-5A, Rip/Rab (nucleoporin-like proteins), and RNA helicase A have been found to interact with the Rev-RRE system, although their precise roles have yet to be investigated (*34-36*).

2.4 Research Objective

Rev-RRE has been chosen for its high binding specificity and affinity in vitro. A portion of Rev and RRE containing the minimum binding sites required for their interactions will be used with the dotLab system to monitor the binding. The Rev-RRE have a tight interaction with a K_d of 0.2 nM (*37*).

The Rev peptide will have a biotin group attached to its N-terminus and will be bound to the sensor surface via the streptavidin-biotin interaction. The RRE RNA will be washed over the sensor surface once the binding of Rev has occurred. The aim of the study is to successfully monitor the real-time binding of RRE to the immobilized Rev peptide, from which the kinetic data may be extracted. The dotLab system is primarily used for the study of larger molecules, and the main goal of this study is to test whether its application can be

extend to smaller molecules. The use of the dotLab system will then be applied to a novel virus, the Flock House virus, to aid in the identification of RNA sequences involved in genome packaging, discussed further in Chapter 3. A truncated Rev (23 residues) and RRE (30 nucleotides) containing the high affinity binding sites will be used to test the sensitivity of the dotLab system (Figure 2.3). The RRE RNA has been modified for stability, without affecting binding efficiency, and has been used in previous NMR studies; two extra bases were added on stem IID, and the hairpin loop was changed to a more stable UUCG tetraloop. The Rev peptide contains a highly positive overall charge and is able to bind many RNA molecules unspecifically, by measuring the relative association rates (k_{ON}) with the dotLab system; specific binding to the RRE RNA should be visible in the k_{ON} rates compared to unspecific binding of competitor RNAs.

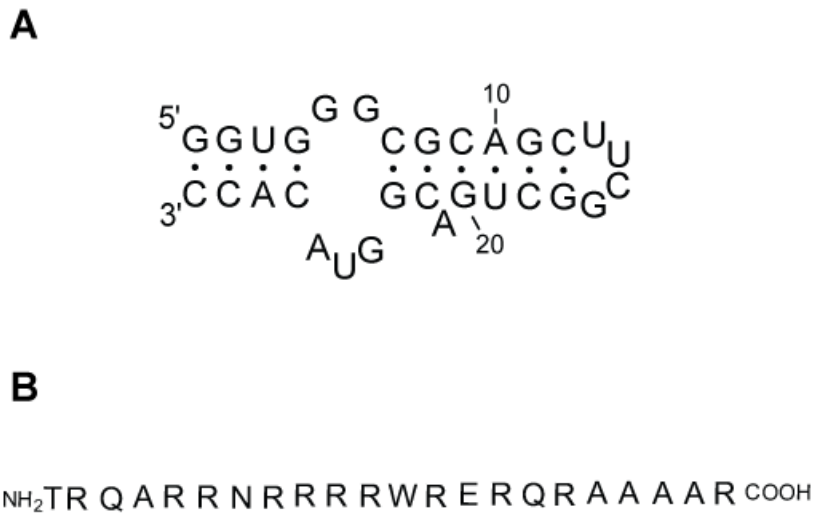

Figure 2.3- Minimum high affinity binding and specificity regions used in the binding study. (**A**) RRE, and (**B**) Rev.

2.5 Materials and Methods

2.5.1 Minimization of RNase Contamination

A number of precautions were taken to minimize RNase contamination during RNA production. Fresh gloves were worn at all times. All preparation areas were wiped with RNase AWAY™. All buffers were made from nuclease-free Milli-Q water and autoclaved. All the labware used was wrapped in aluminum foil and autoclaved at 121 °C; prior to use, it was washed with RNase AWAY™ followed by rinsing 3X with nuclease-free Milli-Q water. All plastic-ware utilized was RNase free certified by their respective manufacturers. During RNA synthesis reactions RNase inhibitor was added.

2.5.2 RNA Template Preparation

The DNA template was prepared by combining the bottom strand with the top strand DNA. The bottom strand contains the DNA sequence that will serve as the template for RNA synthesis and has the complimentary sequence for the top strand T7 promoter. The top strand is an 18 bp primer that anneals to the promoter region of the bottom strand creating T7 enzyme binding site.

The top strand (5'TAATACGACTCACTATAG 3') and bottom strand (5'GGTGTACCGTCAGCCGAAGCTGCGCCCACCTATAGTGAGTCGTATTA 3') DNA oligos were obtained from Sigma Aldrich. Lyophilized pellets of each strand are resuspended in nuclease free water (nf. water) to make a 100 µM solution. A 20 µM template solution (20 µM bottom strand, 30 µM top strand, 10 mM Tris pH 8.0, and 10 mM $MgCl_2$ final concentration) is prepared by heating at 95 °C for 5 minutes and chilling on ice for 5 minutes.

2.5.3 Synthesis of RNA

RNA synthesis was performed with the prepared template using the T7 RNA polymerase by means of a runoff transcription. The transcription reaction mixture was set up as described in Table 2.1.

Table 2.1- Transcription reaction mixture.

Solution	Final Concentration
HEPES buffer pH 7.5	80 mM
DTT	15 mM
$MgCl_2$	33 mM
Spermidine	1 mM
rATP, rGTP, rCTP, rUTP	3.75 mM each
20 µM Template	0.5 µM
RNase Inhibitor	1 unit/µL
T7 RNA polymerase	

After the addition of T7 RNA polymerase enzyme the reaction is incubated in a water bath at 37 °C for a total of 6 hours. Once 3 hours have passed half the amount of T7 enzyme and $MgCl_2$ are added. Once 6 hours have passed a white precipitate of magnesium pyrophosphate should be observed. The reaction is spun at maximum speed to pellet the magnesium pyrophosphate. The transcription reaction is transferred to a new container and 0.5 M EDTA is added to sequester any remaining magnesium.

The transcription reaction is ethanol precipitated with the addition of $1/10^{th}$ the volume of 3 M sodium acetate (pH 5.2) and 2.5 times the volume of cold 100% ethanol. The precipitation reaction is left at -80 °C for an hour or 10 minutes on dry ice, followed by centrifugation at maximum speed (4 °C) to pellet the precipitant. The pellet is washed with the total volume of the precipitation using cold 70% ethanol to remove excess salt. The pellet is centrifuged at maximum speed (4 °C). The supernatant is removed and the remaining pellet is placed on dry ice for 10 min. to freeze before placing on the FreeZone Plus 4.5L console system lyophilizer (Labconco) to dry.

2.5.4 RNA Purification

The RNA produced by in vitro transcription is purified using polyarcylamide gel electrophoresis (PAGE). The dried RNA pellet is resuspended in 8 M urea and run on a 12% denaturing polyacrylamide gel containing urea as the denaturant. The transcription reaction is separated on a 14x15 cm gel with the Hoefer SE 400 electrophoresis unit. The RNA resuspended in urea is loaded onto the gel and a separate well is loaded with bromophenol blue and xylene cyanol dyes to monitor the progress of the gel. The gel is finished and may be stopped once the bromophenol blue dye band has almost run off. The RNA transcript product will appear in between the two dye bands and can be visualized by UV shadowing on a silica gel sheet.

The crush and soak method is used to purify the RNA from the gel and the transcription mixture. The RNA band is cut out of the polyacrylamide gel and the gel piece is cut into small pieces. The gel pieces are placed in a 15 ml falcon tube with enough TEN buffer (10 mM Tris pH 7.6, 1 mM EDTA and 0.3 M NaCl) to cover all the gel fragments. The falcon tube is incubated at 65 °C for 10 min. and left shaking for 2 hours to overnight. After the crush and soak, the tubes are spun at maximum speed and the supernatant is carefully transferred to a new tube avoiding transfer of any polyacrylamide. The RNA is ethanol precipitated from the supernatant and resuspended in water.

The purification of the RNA is confirmed on a 12% denaturing polyacrylamide gel stained with 1X SYBR Green II dye. The gel was visualized by excitation at 302 nm with a 537 nm emission filter on the FluoroChem FC2 imaging illuminator coupled with AlphaEaseFC v.6.0 software (Alpha Innotech) The RNA concentration was determined using the NanoDrop UV-Visible spectrophotometer (NanoDrop Technologies).

2.5.5 Purification of Rev Peptide

Crude synthesis of the 23 amino acid Rev (DTRQARRNRRRRWRERQRAAAAR) peptide was obtained from CanPeptide Inc.. 10 mg of the crude peptide were dissolved in 5 mL of nf. water with 10% acetonitrile. The solution was spun at 13 000 rpm for 30 minutes, before injecting into an HPLC system. The peptide was purified by reverse phase high pressure liquid chromatography (RP-HPLC) on a Waters HPLC system. Vydac C18 column (5 µm 300Å, 4.6x100mm) (Grace) was used for purification and elution was achieved with a linear gradient from 10 to 60% of solvent B (100% acetonitrile 0.04% TFA) in solvent A (0.1% TFA) over 40 minutes at 1 mL/min flow rate. Absorbances were monitored at 220 nm and 280 nm with the Waters 2996 photodiode array detector. The solvents used for the HPLC were filtered using a 0.2 µm membrane filter and degassed. The Rev fraction collected was characterized by electrospray ionization mass spectrometry (ESI-MS). The sample was prepared for ESI-MS by diluting it with a solution containing 1:1 acetonitrile:water with 0.2% formic acid. Once correctly characterized the HPLC fraction was lyophilized and resuspended in nf. water.

The concentration of the recovered peptide is determined using the NanoDrop UV-Visible spectrophotometer (NanoDrop Technologies). The extinction coefficient for the 23 amino acid Rev peptide was determined using the ProtParam tool on the ExPASy (Expert Protein Analysis System) proteomics server of the Swiss Institute of Bioinformatics (*38*).

2.5.6 Labeling and Purification of Rev Peptide

The labeling reaction was set up with 1:5 molar ratio of peptide to biotin as was determined by Selo, I. *et al.* for preferential biotinylation of N-terminal amino groups in peptides. The biotin N-hydroxysuccinimide ester (BNHS) (Sigma Aldrich) was dissolved in dry dimethylformamide. The reaction mixture contained 70 nmoles of Rev peptide in 120 µL phosphate buffer (50mM, pH 6.5) followed by the addition of 350 nmoles of BNHS (9.5

μL). The final concentration of organic solvent should be below 20% in the reaction mixture. The reaction was left at 4 °C for one hour and stopped by acidification with 70 μL of 1% trifluoroacetic acid (TFA). The reaction was qualitatively checked by ESI-MS for the correct product formation before purification. Purification of the biotinylated Rev peptide was performed in the same manner as the purification of the crude synthesis and the concentration was determined on the NanoDrop UV-Visible spectrophotometer (NanoDrop Technologies).

2.5.7 Rev-RRE Binding Assay

The Rev-RRE binding assay was performed and monitored on the dotLab system (Axela Inc.). The dotLab system software version 1.0.12.15 was used to write the methods that would be executed by the instrument. A general procedure used to load the samples onto the sensors is outlined in Figure 2.4. The dotLab sensors already contain avidin covalently attached to the surface. The sensors were taken from the 4 °C storage and were allowed to come to room temperature (~1 hour) before use. All the washing steps in the method were performed with the 1X phosphate buffered saline (PBS) solution (137 mM NaCl, 2.7 mM KCl, 10 mM Na_2HPO_4, 2 mM KH_2PO_4, pH 7). The 1X PBS solution was used to dilute all the samples to their final concentration prior to each run. The RRE RNA sample was heated for 1 minute at 95 °C and immediately placed on ice and cooled for 5 minutes before loading onto the sensor. In order to ensure the RNA integrity in the binding assays, the RNA was mixed with 1X PBS solution and incubated for 2 hours and analyzed by PAGE.

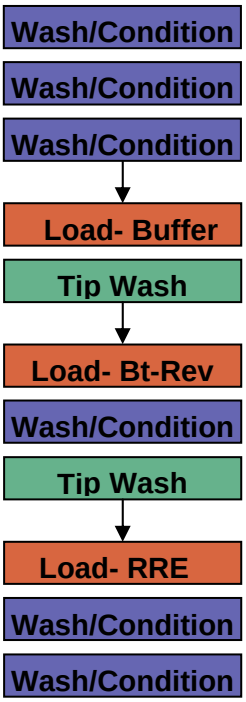

Figure 2.4- General method for Rev-RRE binding assay to the dotLab sensor.

2.5.8 Software

The RNA secondary structure figures were generated using mfold v.3.2 an RNA secondary structure prediction program, along with RnaViz v.2 software for producing RNA secondary structure drawings (*39-41*). Peptide sequences were made using ChemBioDraw Ultra 11.0 (CambridgeSoft).

2.6 Results and Discussion

2.6.1 Production and Purification of RRE

In-vitro transcription with T7 polymerase along with the constructed template (top strand + bottom strand) was used to synthesize the 30 bp RRE RNA. The success of the transcription reaction and purification was verified using a 12% denaturing polyacrylamide gel stained with SYBR Green II dye, which has a higher binding affinity for RNA than DNA, and shows fluorescence enhancement upon binding RNA. The result of the transcription and purification are shown in Figure 2.5. Lane 2 and 3 have only the DNA template loaded that is in total 65 bp (18 bp top strand + 47 bp bottom strand). The polyacrylamide gel contains urea as a denaturant that causes the template DNA to separate into single-strands. This is why only the bottom strand (47 bp) is visible on the gel and the top strand (18 bp) fragment has run off the gel with abortion products and free nucleotides. The lanes 6 and 7 show unpurified 50 µL transcription reactions producing the correct size RNA. The abortion products and nucleotides have run off, although some are still present and seen as a streak down the gel. Samples of the smaller transcription reaction were kept to run as comparisons with the purified sample. RRE RNA was purified by UV-shadowing and cutting out the correct band corresponding to the RNA, followed by a crush and soak and ethanol precipitation to obtain the purified RNA. Lane 9 of the polyacrylamide gels shows the successfully purified RRE RNA obtained from a 3 mL transcription reaction, with no contamination of either DNA or RNA.

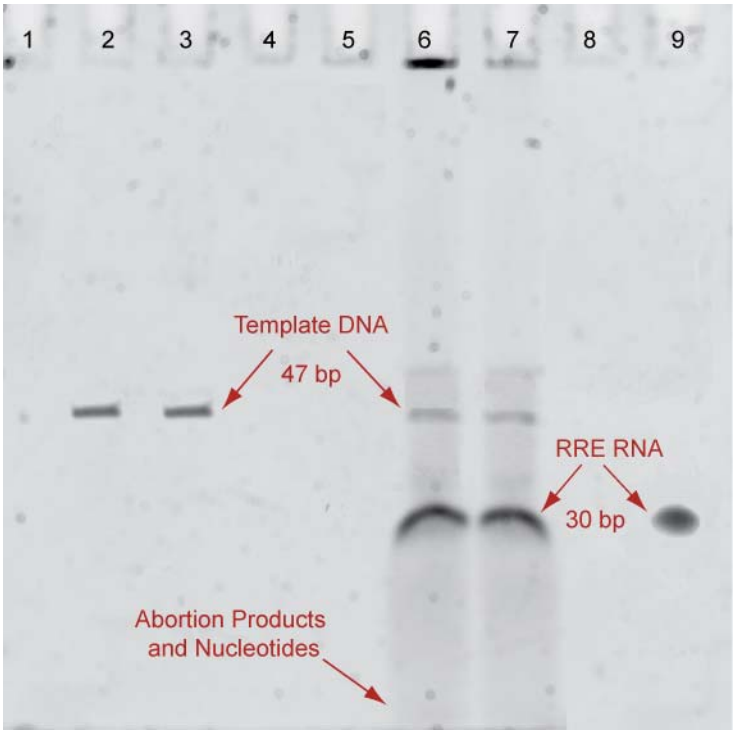

Figure 2.5- Transcription and Purification of the RRE RNA. 12% denaturing polyacrylamide gel stained with SYBR Green II showing the result of the transcription reaction and the success of the purification.

2.6.2 Purification of Rev peptide Crude Synthesis

Crude synthesis of the Rev peptide obtained from CanPeptide Inc. was purified by RP-HPLC to remove peptidic by-products. The crude peptide was dissolved in 10% acetonitrile before loading on a C18 column that separates molecules based on their hydrophobicity, with the most hydrophobic molecules eluting last. The elution was done with a linear gradient from 10% to 60% of solvent B. The elution profile of the crude synthesis of the Rev peptide is shown in Figure 2.6.

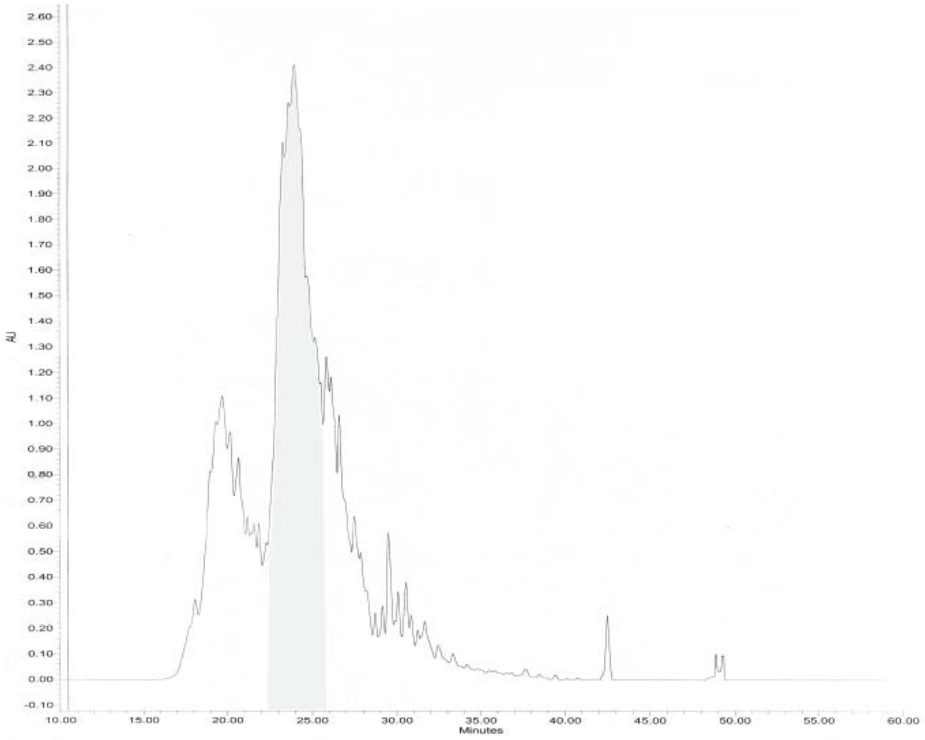

Figure 2.6- Purification of the Rev peptide by RP-HPLC.
The gray area under the peak corresponds to the collected fraction containing the Rev peptide. The elution process shown was monitored at 220 nm.

The eluted fraction was further characterized by positive ion mode ESI-MS. The molecular mass of the Rev peptide obtained through MS was in agreement with the expected molecular mass of 2993 Da (Figure 2.7). The obtained molecular mass of 2992 Da reflects the loss of a hydrogen atom that occurred during MS; however it still confirms that the full-length Rev peptide has been purified.

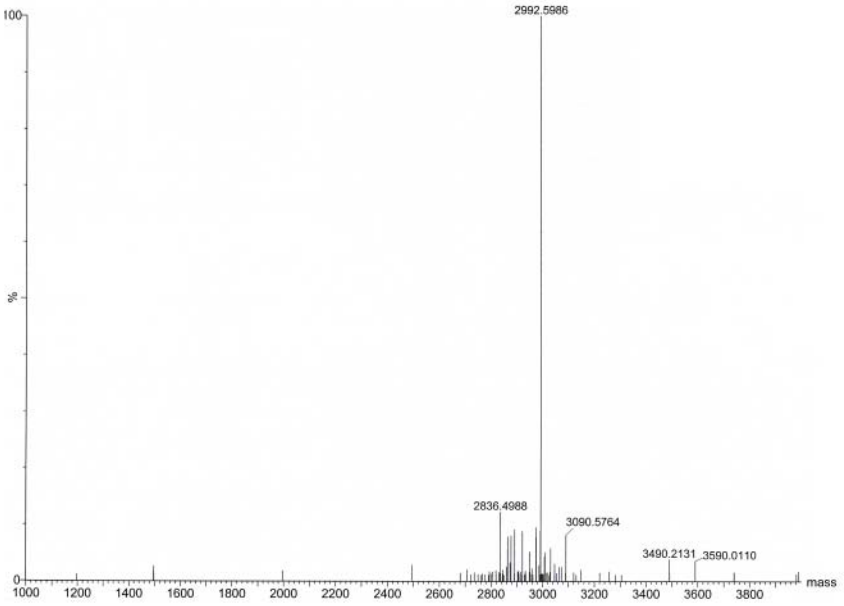

Figure 2.7- Positive ion mode ESI-MS of the purified Rev fraction. The 2992 Da major peak belongs to the Rev peptide and differs by a hydrogen atom from the calculated mass of 2993 Da.

2.6.3 Biotinylation of the Rev peptide

The biotinylation reactions can be used to label proteins with a biotin moiety by exploiting NHS ester and primary amine chemistry. Primary amines react with NHS ester to form stable amide bonds. The reaction only works with amines in their non-protonated form. The reaction can be made selective by controlling the pH, thus affecting which amine groups (N-terminal, lysine side-chain) are predominantly reacting. The biotinylation reaction was performed with a 1:5 molar ratio of the Rev peptide to biotin N-hydroxysuccinimide ester (BNHS) (Figure 2.8). The labeling reactions were allowed to go for 30 minutes and 1 hour before stopping. It was found that the labeling reaction was rapid for the Rev peptide; as a result longer reaction times were not tested. After the reaction was stopped with 1% TFA, a 5 µL aliquot was removed to be analyzed by MS. MS was performed to determine qualitatively if the Rev peptide has been labeled before beginning purification (Figure 2.9).

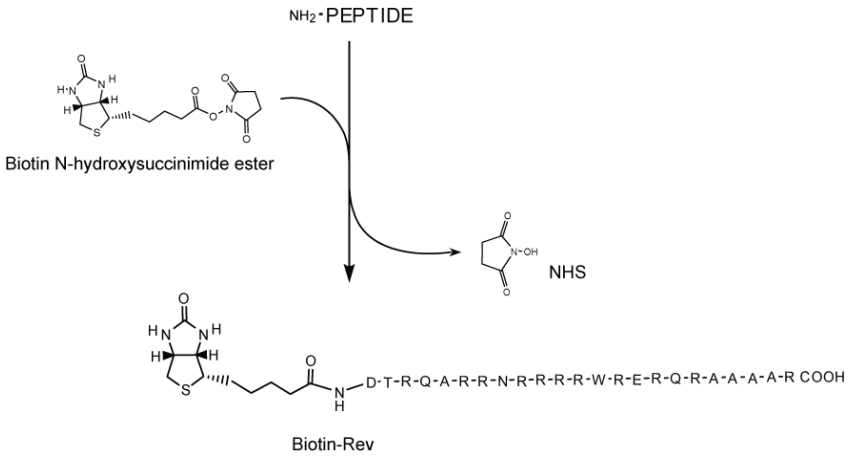

Figure 2.8- Rev biotinylation reaction scheme.

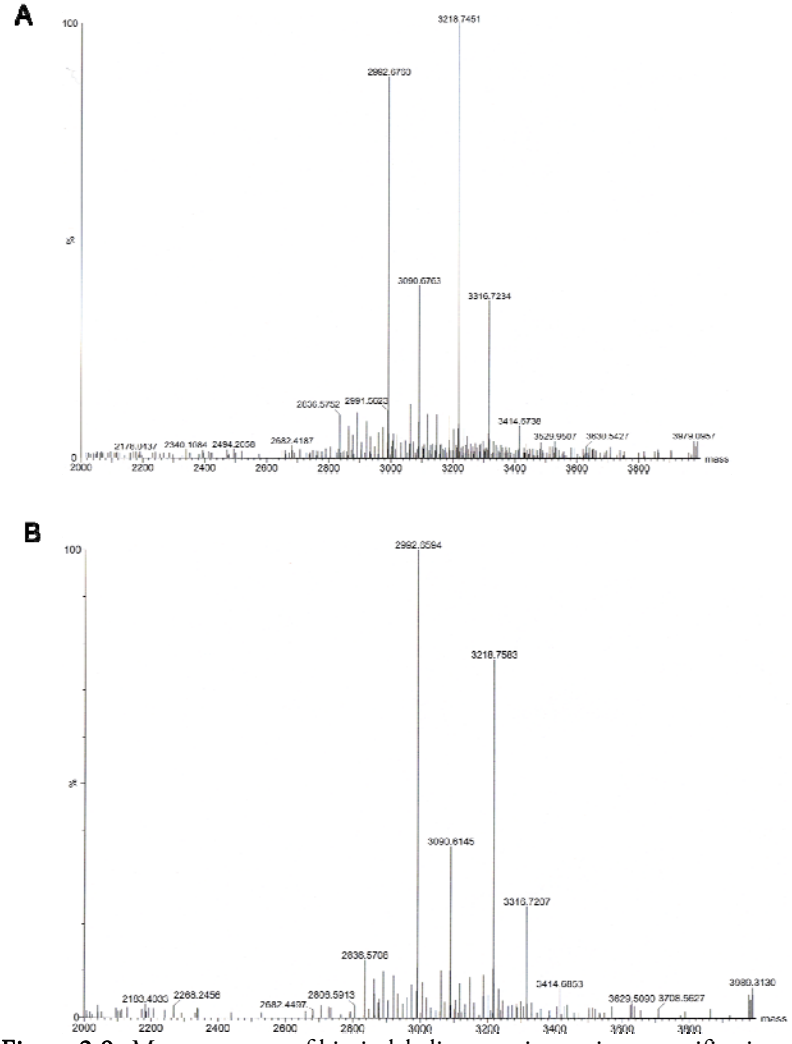

Figure 2.9- Mass spectrum of biotin labeling reactions prior to purification. (A) Labeling 30 min incubation time, (B) labeling 1 hour incubation time.

The purification of the biotinylation reaction was carried out as the correct mass was visible in the mass spectrum for the labeled Rev peptide. The labeling reactions were purified by RP-HPLC on a C18 column. To the 30 min and the 1 hour reaction 10% acetonitrile was added before loading the column, followed by elution using a linear gradient from 10% to 60% of solvent B. The RP-HPLC elution profiles for the 30 minute and 1 hour labeling reaction are shown in Figure 2.10.

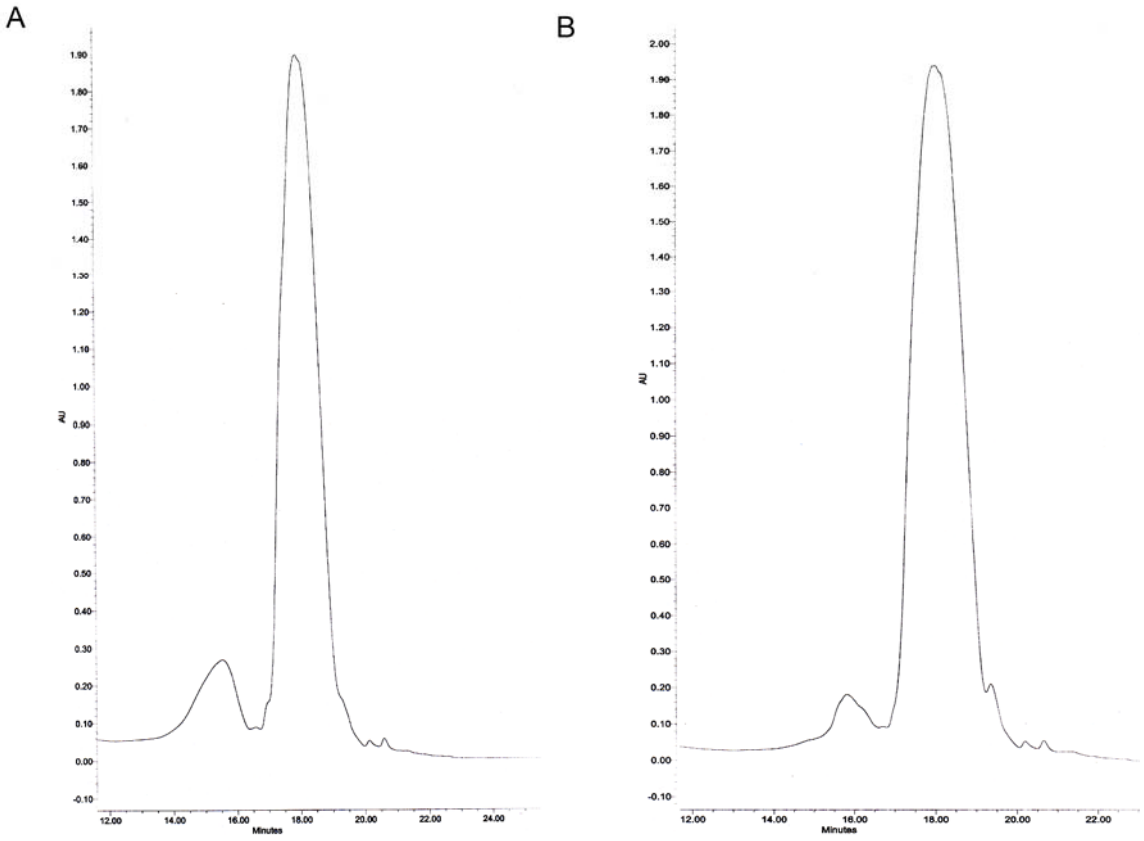

Figure 2.10- RP-HPLC elution profiles of 30 min. and 1 hr. Rev Biotin labeling reactions.
(A) 30 min. labeling reaction with two eluting fractions at ~16 and 19 min.
(B) 1 hr. labeling reaction with two eluting fractions at ~17 and 19min.

The elution profiles for the two reaction times are similar with the minor difference being the slight variation in elution times. The amount of unlabeled peptide is also greater in the 30 minute reaction compared to the 1 hour reaction time. The two peaks in the

chromatograms have both been characterized by MS (Figure 2.11). The first peak in the 30 minute reaction eluting approximately at 16 minutes corresponds to the unlabeled peptide (2993 Da) with some labeled product present. The second peak eluting at approximately 19 minutes is the N-terminally labeled Rev peptide with a mass of 3219 Da. MS analysis of the 1 hour reaction chromatogram peaks were found to be analogous to those from the shorter 30 minute reaction time. Labeling and purification of the N-terminally labeled Rev peptide was achieved.

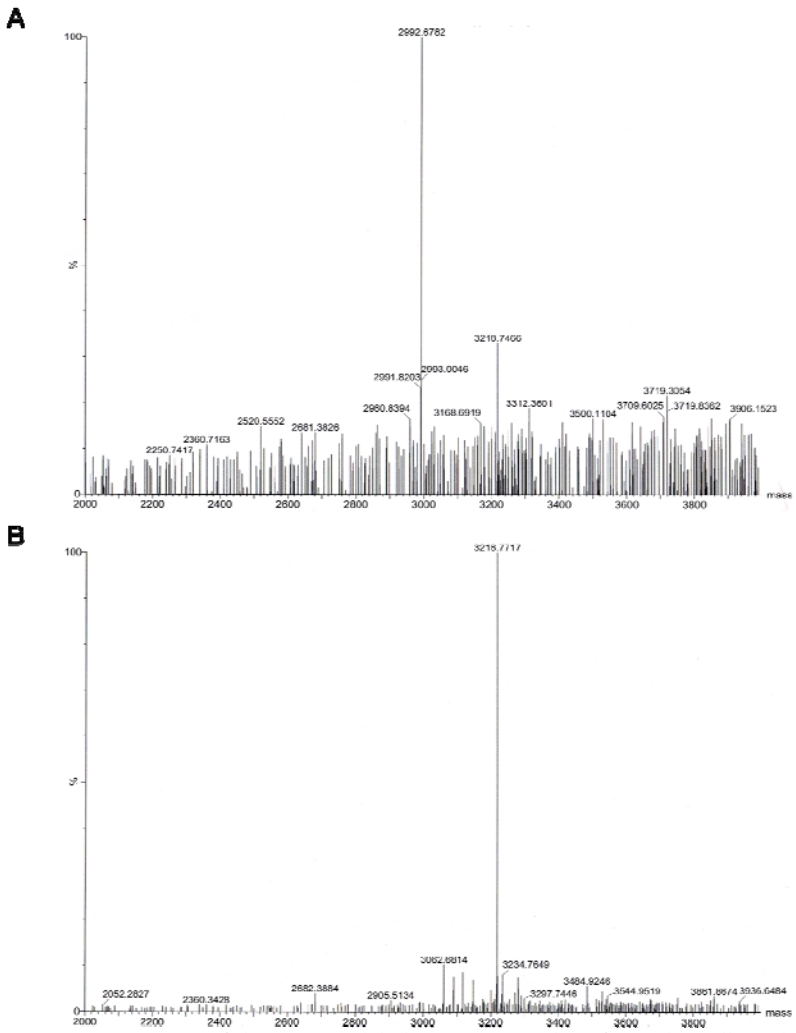

Figure 2.11- Mass spectrum of the 30 min. labeling reaction identifying the collected fractions. (A) Peak fraction eluting at 16 min., major peak (2992 Da) corresponds to unlabeled Rev peptide. (B) Peak fraction eluting at 19 min., major peak (3218 Da) indicates N-terminally labeled Rev peptide.

2.6.4 dotLab Binding Assay

The Rev-RRE system was chosen to test the potential use of the dotLab system in characterizing RNA-protein interactions. In order to study the specific binding of a molecule to its binding partner with this system it is required that one of the components be immobilized on the sensor surface.

In initial binding studies with the Rev-RRE interaction performed on the dotLab system we used the amine reactive sensors. The sensors surface contained carboxyl groups, which when activated with carbodiimide chemistry can couple primary amines of proteins to the surface through amide bond formation. The advantage of using these sensors is that small amounts of protein are required for the coupling reaction. Coupling of the Rev peptide to the amine surface at different concentrations (10 µg/mL and 30 µg/mL) was explored. The reaction carried out in an amine free buffer system to prevent other molecules with a free amine group from binding and competing with the peptide. A 6.5 pH buffer was used to promote the binding to N-terminus of the Rev peptide. The coupling of the Rev peptide did not produce big enough change on the sensor surface and was not detected. Subsequent addition of the RRE after the coupling of Rev did not show any changes in the diffractive index to indicate binding (Figure A1.1). This may have several reasons:

- The Rev peptide may lay flat across the surface upon binding that it does not produce the necessary height change to produce a signal.
- Immobilizing the Rev peptide through the N-terminus in close proximity to its RNA binding site may impair its ability to bind the RRE.
- Steric hindrance can also block the binding sites of neighboring molecules due to the high concentration of immobilized molecules (Rev).

Increasing the distance of the Rev peptide from the sensor surface should allow for better detection of surface binding and aid it in binding the RRE RNA.

The avidin coated sensors utilize the high affinity between biotin and avidin to immobilize molecules of interest to the sensor surface. A single avidin is able to bind up to four biotin

molecules and can act as a signal enhancer; this however is affected by the technique used to immobilize the biotin to the sensor surface (*42*). The biotinylated Rev peptide contains a short linker region that will provide increased distance from the sensor surface (Figure 2.12).

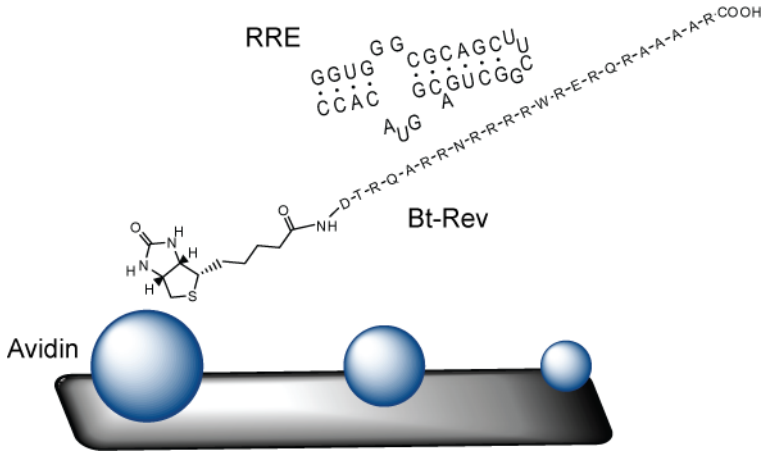

Figure 2.12- Avidin sensor binding depiction of Bt-Rev-RRE.

The avidin sensor binding assays performed with the Biotin labeled Rev and the RRE counterpart are summarized in Table 2.1. The first binding assay involved a basic method used by Axela to bind large antigen/antibody molecules. There was a large increase in the diffractive index upon binding of the biotinylated Rev peptide (Bt-Rev), but no increase was observed for the binding of the RRE. Increasing the RRE incubation period and the concentration mixed over the sensor was unsuccessful at producing visible binding (Figure 2.13). Lower Bt-Rev concentrations and incubation times were investigated, as surface crowding and steric hindrance were believed to be preventing RRE binding. The RRE RNA was heated at 95 °C and quickly cooled on ice to minimize formation of duplex and to promote hairpin structure formation. A 30 second incubation of Bt-Rev (3 µg/mL) along with a 5 minute incubation with previously heated RRE RNA (95 °C) produced a change in the diffractive index most likely corresponding to binding (Figure 2.14).

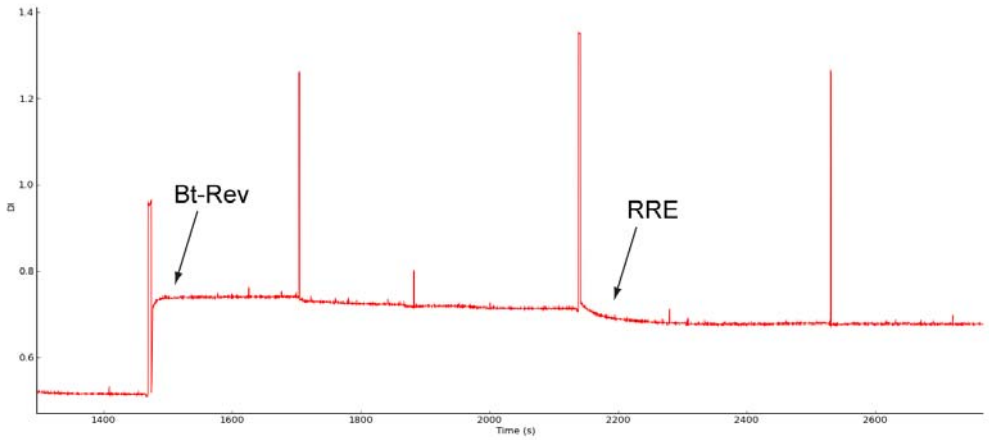

Figure 2.13- Binding assay performed with high concentration of Bt-Rev-RRE. The data represent the second binding assay from Table 2.1.

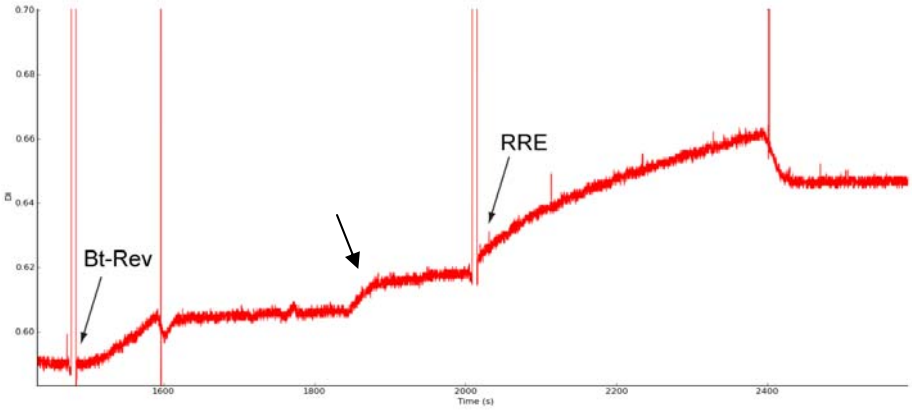

Figure 2.14- Binding of RRE to surface immobilized Rev monitored by change in the DI over time. The variables changed that led to observing RRE binding are outlined in Table 2.1 under assay number 5.

In order to determine if indeed crowding at the surface was interfering with RRE binding or if it was the RNA secondary structures was examined by increasing the Bt-Rev incubation period. This yielded no binding of RRE. If RNA secondary structures were responsible for observing no binding, then heating the RNA at higher temperature would have resolved this possibility. The reagent flow rates and incubation times were changed to attempt to increase the change in the diffractive index for Bt-Rev, thereby increasing the RRE signal as well. Binding was observed for RRE although the change in surface height was lower than previously obtained (Figure 2.15). These results show that high concentration of immobilized Bt-Rev at the sensor surface hinders the binding of the RRE RNA. The binding

of RRE to Bt-Rev has only been observed when the diffractive index change for the binding of Bt-Rev is less than 1 DI. In Figure 2.14, the jump in DI during the washing step (indicated by the arrow) after Bt-Rev incubation is believed to be the peptide that was stuck to the fluidic tubing and has come off in the wash. The negatively charged sensor surface could be contributing to the difficulty of immobilizing the Rev peptide. The Rev peptide contains many positively charged arginine groups that may interact with the negatively charged sensor surface and cause the peptide to be in an orientation where it cannot bind to the RRE. The addition of a BSA blocking step may minimize surface interactions with the sensor surface and the fluidic tubing. Due to the large size of BSA it could also promote crowding of the peptide. The Rev peptide can be labeled with Biotin-X-X-NHS that has a 14 atom spacer region and would provide additional height on the sensor surface and may promote more favorable binding interactions. Therefore, it seems that the dotLab system is sensitive enough to detect the binding interaction of a small 23 amino acid peptide and a 30 nucleotide RNA.

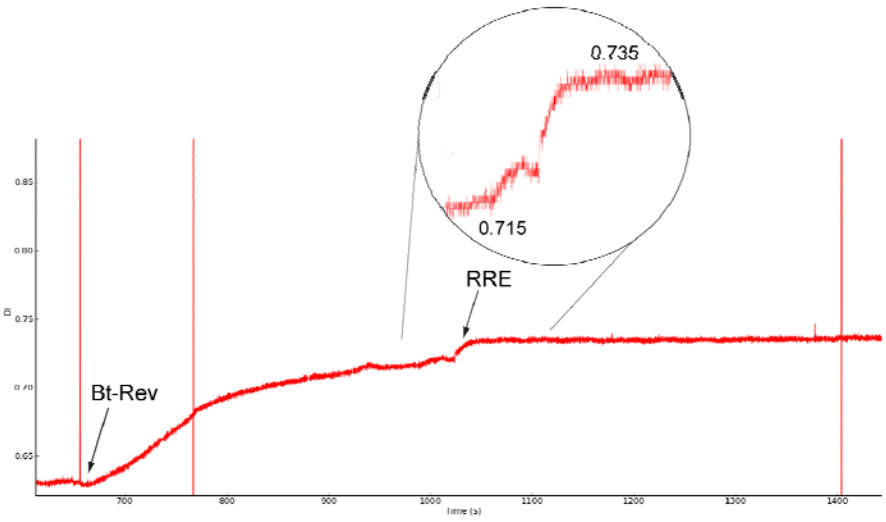

Figure 2.15- Monitoring the DI change upon binding of the RRE with longer incubation times. The variables changed are found in Table 2.1 under assay 7. A higher surface area concentration of Rev did not translate into an increased signal for RRE binding.

Table 2.2- Summary of the variables changed in the Rev-RRE binding assays.

Binding Assay	[Bt-Rev] µg/mL	Incubation Duration (min:sec)	[RRE] µg/mL	Incubation Duration (min:sec)	Additional Changes
1	60	2:00	50	3:00	
2	60	0:30	80	5:00	
3	10	0:30	50	5:00	RRE heated at 65 °C
4	5	0:30	50	5:00	
5	3	0:30	50	5:00	RRE heated at 95 °C
6	3	1:20	50	5:00	
7	3	0:50	50	5:30	Changed flow rates
8	3	0:50	50	5:30	Changed flow rates
9	3	0:30	50	5:30	Changed flow rates
10	1	0:10	50	5:30	

Chapter 3: Flock House virus

3.1 Introduction

Flock House virus (FHV) was discovered on the North Island of New Zealand, and was isolated from the New Zealand grass grub *Costelytra zealandica* (White beetle) (*43*). The grubs were alive when found, but it appeared that the virus hindered their development. FHV was shown to have a cytopathic effect (CPE) on *Drosophila melanogaster* cells and caused characteristic cell clumping, although complete lysis of the cells was not observed. The CPE and the physicochemical properties indicated that FHV is a unique new emerging insect virus belonging to the *Alphanodavirus* genus in the *Nodaviridae* family. FHV is able to replicate in several insect species, plants and yeast; no CPE effects were observed in mammalian cells and hence it is not considered a human pathogen (*43, 44*).

FHV is a nonenveloped positive single stranded ((+) ssRNA) virus which contains a bipartite genome. The virus replicates in the cytoplasm of infected cells. The genome is made up of two 5' ^{m7}G-capped, nonpolyadenylated RNA's (RNA1 and RNA2) which are both packaged into a single virion (*45, 46*). RNA1 (3.1kb) encodes protein A (112 kDa), the RNA-dependent RNA polymerase (Rd-RP) found on the outer mitochondrial membrane of infected cells (*47*). RNA2 (1.4kb) encodes protein alpha (43kDa), a capsid precursor protein (Figure 1). Protein A has been shown to play a role in recruiting RNA1 to the RNA replication site (*47*). RNA1 also gives rise to a subgenomic RNA3 species, located near the 3'- terminal end of RNA1 and consisting of 387 nucleotides. RNA3 encodes protein B2 (10 kDa) which plays an important role in countering the RNAi defensive mechanism of the host (*48*). Protein alpha along with RNA 1 and RNA2 initially assemble into a noninfectious precursor particle called a provirion. The provirion matures and develops infectivity by spontaneous cleavage of the 407 amino acid protein alpha between the residues Asn 363 and Ala 364 to produce two proteins, beta (38 kDa) and gamma (5 kDa) (*49, 50*).

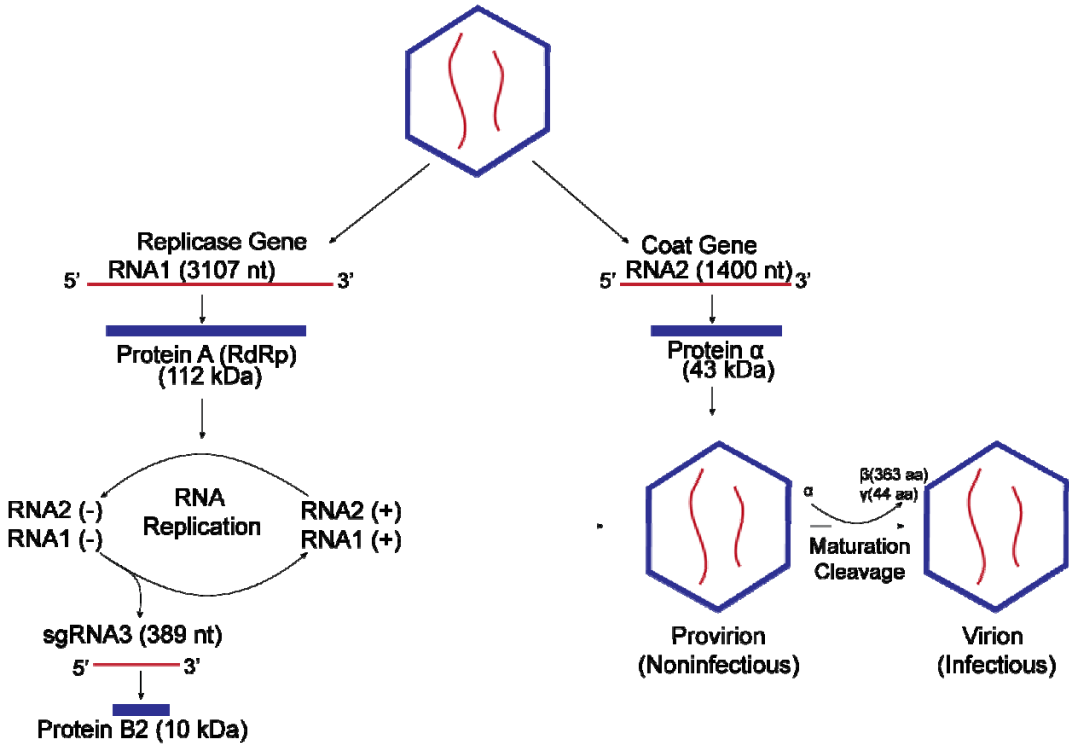

Figure 3.1- Formation of Flock House virus (see text for details).

3.2 Flock House virus Structure

Until recently, the structural study of (+) ssRNA insect viruses was difficult due to the need for milligram amounts of intact virus for crystallization (*51*). Many viral protein capsids have icosahedral symmetry, since it is the most efficient way to obtain a symmetrical shell with a maximum internal volume using asymmetric proteins (*1, 9*). The smallest number of identical protein subunits needed to construct the icosahedral capsid is 60 (*1*). These subunits are positioned in such a way that they are interconnected through the two-, three- and five-fold rotational axes that denote the icosahedral symmetry (*1*). Most viruses have capsids that are comprised of more than 60 subunits and, in order to understand how the icosahedral symmetry is maintained, one needs to look at the concept of quasi-equivalence by Caspar and Klug (*51*).

The quasi-equivalence theory states that each protein subunit that makes up a larger capsid consisting of more than 60 subunits is found in different structural environments with similar bonding properties (*1, 52*). Facets are composed of protein subunits found in different environments that make up the new asymmetric unit (*1*). The triangulation number (T) of a viral capsid describes the number of protein subunits needed to form the asymmetric unit that make up the capsid (*1*). The combination of the smaller triangular asymmetric units (facets) enables the capsid to retain its icosahedral symmetry.

The FHV capsid consists of 180 protein subunits, which give rise to 60 triangular facets and a capsid icosahedral symmetry of T=3 (180/60=3) (Figure 2a) (*53*). The 60 triangular units are composed of three identical protein subunits (A, B and C), which consist of an eight-stranded antiparallel β sandwich that is conserved among Nodaviruses. It should be noted that although there is structural conservation, the amino acid sequence is not conserved among the different species (*53*). The 3.0Å crystal structure of FHV reveals an RNA A-type duplex forming only at the two-fold axis of symmetry (*53*). The RNA duplex is ordered only between two C subunits of opposing orientation (C- C2) (Figure 2a). The RNA sugar phosphate backbone interacts with the subunits through electrostatic and van der Waal forces (*53*). The N-terminus of all three identical protein capsid subunits contains lysine and arginine residues and inserts into the major groove of the RNA duplex to help neutralize the negative charge of the RNA backbone (*53, 54*). RNA's role is to prevent the bending of the two subunits and form a flat contact (*53*). The 10 ordered base pairs make up 20 % of the packaged genome of RNA found at each of the two-fold axes (*53*). The γ –peptide produced as a result of maturation cleavage of the provirion is located inside the capsid interior as an alpha helix (*53*). The γ_C and γ_B helices of the C and B capsid protein subunits interact with the ordered RNA duplex (*52*). The γ_A helix does not interact directly with the RNA duplex but may play a role upon interacting with the cell receptor or a membrane (*52*).

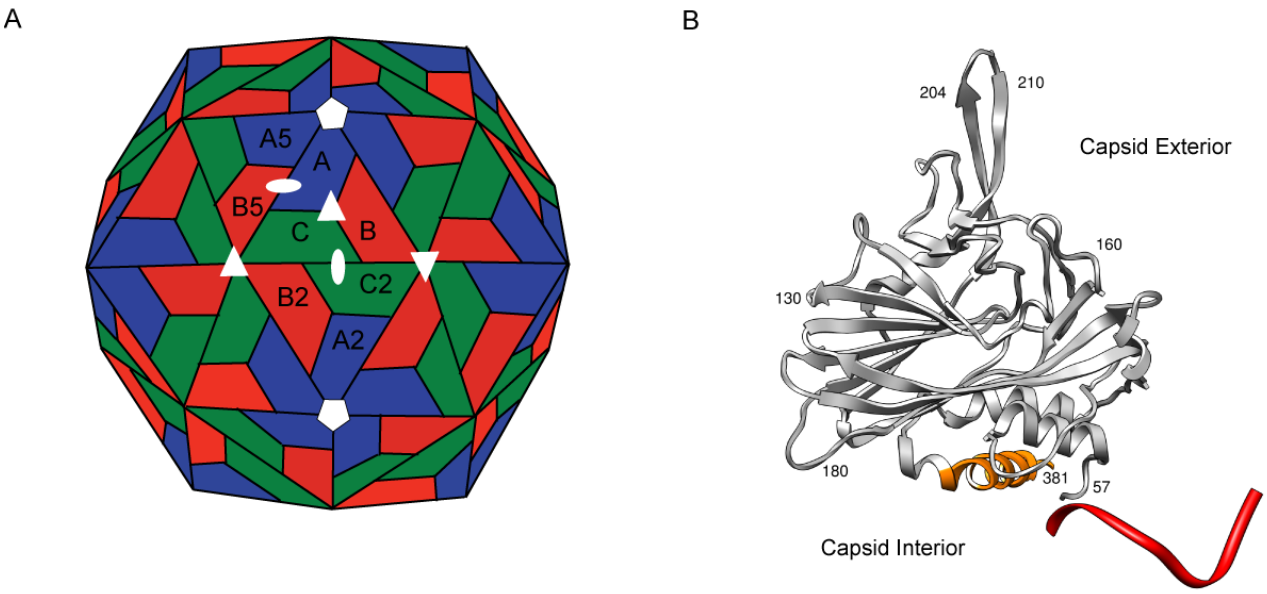

Figure 3.2-Flock House virus structure and RNA-protein subunit interaction.
(**A**) Capsid structure of FHV with T=3 symmetry. Three identical protein subunits make up the larger facet (A, B and C). The two, three and five fold axes are distinguished by an oval, triangle and pentagon, respectively. The dsRNA lies between the C-C_2 subunits. (**B**) The tertiary structure of the C subunit of FHV. Residues 1-54 of the N- terminus are disordered in the electron density; as well as the C-terminus residues 382-407. The maturation cleavage product the γ –peptide is shown as an orange alpha helix. A portion of dsRNA is shown as a red ribbon interaction with a portion of the N-terminus. (PDB ID# 2Q25)

3.3 Method of Cell Entry

The cell puts up quite a challenge for viruses attempting to release their genetic information into it, putting up complex barriers which the virus must overcome. These barriers consist of the plasma membrane as well as many intracellular membranes (*55*). The last membrane the virus must penetrate in order to begin its life cycle and form new progeny is referred to as the limiting membrane (*55*). The exact method of delivery has not been as well determined for nonenveloped viruses as it has for enveloped viruses, which are known to be able to fuse their viral membrane with the cell membrane, allowing them to penetrate the cell (*55*). Nonenveloped viruses have developed different methods of delivering their genome into the target cells as they do not have a surrounding lipid bilayer. The capsid of nonenveloped viruses must be sturdy enough to handle the harsh environment extremes (pH, ionic strength, temperature and proteases) until it reaches its limiting membrane (*56*). The viral

capsid must be able to react only with the appropriate cellular factors that will result in a conformational change and allow it to interact with the limiting membrane. The stability and conformational change of the viral capsid are believed to be key attributes in the assembly of the virion. During assembly, the viral capsid proteins fold into a provirion structure. Cleavage follows. The formation of a precursor structure gives the possibility that the lowest energy states differ between precursor and product. The formation of the provirion then traps the virus in a metastable state, and the lowest energy state of the mature virion is blocked due to an energy barrier (*56*). Binding to a host receptor then triggers the lowering of the activational energy needed to reach the lowest energy state for the mature virion and hydrophobic residues required for membrane attachment are displayed on the viral capsid.

Infection of host cells by nonenveloped viruses follows a four step process: 1) the movement of the virus to the site of entry; 2) a conformational change induced by cellular factors (receptors, low pH, proteases or chaperones) that release a viral protein (VP) or make a portion of the capsid hydrophobic; both in turn are responsible for interacting with the membrane; 3) the binding of the hydrophobic residue or the VP to the limiting membrane of the host; and 4) the disruption of the lipid bilayer to transport the viral particle or the genome across the membrane (*55*).

The cell entry pathway for FHV has not been fully determined, but current research suggests the pathway is similar to that of other (+) ssRNA viruses, more specifically to the poliovirus, a member of the *Picoronavirus* family. The poliovirus receptor (Pvr) located on the plasma membrane has been found to induce an irreversible conformation change in the viral particle (*55*). This change initiates the penetration process through the exposure of VP 4 and the N-terminus of VP 1 (*55, 56*). VP 1 and 4 are able to insert and bind the plasma membrane (*55*). This binding causes the integrity of the membrane to diminish by forming a channel through which the viral genome may be injected into the cell (*55*). Viral particle breathing occurs at physiological temperatures. It is a process whereby temporary, completely reversible

exposure of viral proteins (VP 1 and 4 from poliovirus) required for membrane attachment are displayed on the capsid surface (*56*). The breathing in the poliovirus shows the dynamic nature of the capsid and alludes to the irreversible change which the particle will undergo in the presence of a receptor (*56*). Particle breathing was also found to occur in the FHV capsid (*57*). The poliovirus formed distinct particles that acted as intermediaries during cell entry when the virus was subjected to a binding assay of *Drosophila* cells (*58*). The particles are formed once the virion has dissociated from the membrane receptor. The eluted poliovirus particles were found to have an altered capsid structure and different physicochemical properties due to the absence of the VP4 subunit (*58*). Specifically, those poliovirus particles retrieved from the binding assay were unable to rebind to the Pvr (*58*). FHV likewise formed distinct intermediate particles in the same way as poliovirus does, with a portion of their γ-peptide missing (*58*). The FHV particles identified in the binding assay may represent an intermediate stage in the cell entry pathway while the virus is adhering to the membrane (*58*).

A common feature among all Nodaviruses is the cleavage of the provirion capsid proteins to produce an infectious viral particle (*59*). FHV undergoes this cleavage reaction to produce the major capsid protein subunit β and the 44 amino acid residue peptide γ (*49*). The γ-peptide is located inside the capsid after the cleavage reaction and has shown the ability to integrate into the lipid bi-layer (*60*). The first 21 residues of the N-terminus of the γ-peptide partition into the lipid bilayer and increase membrane permeability, as observed with fluorophore release from liposomes (Figure 3) (*61, 62*). The N-terminal region has a hydrophobic nature, with a stretch of amino acids with short side chains, a common feature of fusion peptides in enveloped viruses (*63*). Measurements of membrane binding energy for the N-terminal portion of the γ- peptide revealed that the energy is analogous to that of natural membrane binding toxins and antibacterials (*63*). The high affinity of the γ-peptide to the membrane supports its role in membrane binding and transmembrane passage of viral RNA (*63*). The C-terminal of the γ-peptide is involved in viral RNA recognition and

packaging (*59*). As previously mentioned, only the γ_B and γ_C helices are in direct contact with the RNA duplex; the γ_A helix contacts the RNA only through its carboxyl terminus (*52*). The γ_A helices form pentameric bundles at the five-fold axis of symmetry through the interactions of their hydrophilic sides. The γ_A helices form a potential channel with a hydrophobic surface and a hydrophilic core that can be used for the γ-peptide bundle's escape (*52*).

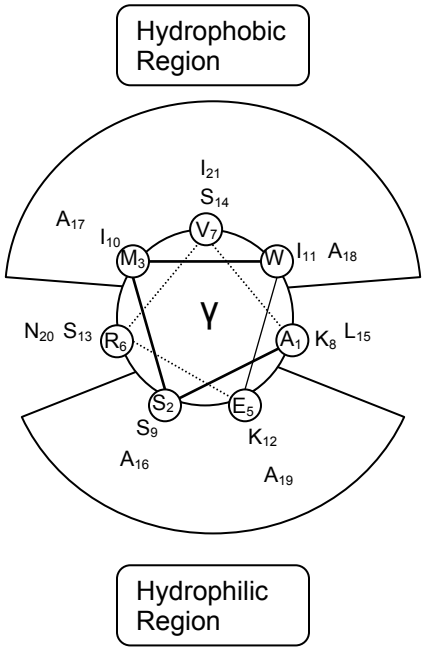

Figure 3.3- Helical wheel representation of the first 21 residues of the γ- peptide.

The current proposed mechanism for the FHV interaction with the membrane or upon binding a receptor is that the subunits along the five-fold axis become destabilized, which allows the γ_A pentameric bundle to surface. The surfacing of the pentameric bundle also pulls the RNA along due to the C terminus interactions. Once the γ_A helix reaches the membrane, further interaction occurs with initiation of the invagination process or creation of a channel for injecting the viral RNA. Poliovirus showed the release of its VP1 subunits upon heating; the same amino terminus was exposed during binding. The same approach was used for FHV; once FHV was heated to 65° C, the γ_A bundles were released along the

pentameric axis regions (*52*). Interestingly only a single protrusion was observed for the FHV capsid, which awaits characterization.

3.4 Eluding the Host Defenses

Many plants and insects have developed silencing pathways as a means to combat viral infections. The RNA interference (RNAi) pathway utilizes the RNase III enzyme (Dicer) that cleaves dsRNA into small interfering RNAs (siRNA) (*48*). The lengths of the siRNAs are between 19-21 base pairs (bp) and also contain 5'phosphates and 3'-two nucleotide overhangs (*48*). The siRNAs are incorporated into the RNA-induced silencing complex (RISC), which is then guided to degrade single stranded RNA molecules (*48*). The RNAi pathway is not only used in the case of viral infections. The ability of Dicer to cleave RNA that contains stem loop structures and generate micro RNAs was shown to have implications in the growth and development of cells (*48*).

FHV encodes an RNAi suppressor protein, B2, a subgenomic RNA expressed from the 3' end of RNA1. The level of B2 expression is highest upon infection and during the replication stage of the virus (*64*). A B2 monomer contains three alpha helices, which combine with another monomer to form a four-helix bundle through antiparallel association (*48*). This B2 dimer binds the dsRNA by recognizing two adjacent minor grooves and inserting itself into the major groove where it interacts with the ribose-phosphate backbone. In a cleavage assay, the addition of B2 completely inhibited the cleavage of a 35 bp dsRNA fragment by Dicer. The B2 protein was also modeled on longer dsRNAs, which suggests that it may prevent the silencing pathway at two key steps. By binding long dsRNA and siRNAs, B2 protein can prevent Dicer from cleaving the viral genome and prohibits the incorporation of siRNAs into the RISC. Transgenic *Drosophila melanogaster,* made to express viral RNA1 and RNA2 but not RNA3 (required for B2 production), showed significantly reduced viral replication and overall production (*64*). Elimination of B2 expression showed that B2 is

required for viral infection. B2 as a means to prevent RNA silencing has been used by FHV to infect multiple hosts: plants, insects and worms.

3.5 Formation of Progeny

3.5.1 RNA Translation

FHV has a (+) ssRNA genome which has the same polarity as mRNA. This feature of positive stranded viruses makes them extremely infectious, since once the penetration of the cellular membrane has occurred, the virus may begin translating the viral genome and replicating shortly after (*65*). Translation of FHV genome occurs before replication, as RNA1 encodes an Rd-RP required for replication. A recombinant baculovirus system was used to show that only coat proteins translated from replicating RNA packaged RNA1 and RNA2 (*66*). Non-replicating RNA1 and RNA2 transcripts produced coat proteins which packaged cellular RNA. Uncoupling protein synthesis from RNA replication showed that the RNA2 can be packaged without the presence of RNA1 only if the capsid protein is translated from a replication-competent RNA2 (*66*). The discrimination of differentially translated coat proteins supports the notion that coat protein translation takes place in specific cellular compartments (*67*). The FHV coat protein is highly basic and it was observed that the coat protein can assemble around cellular RNA with similar efficiency as with viral RNA. The use of cellular compartments by viruses would confine the coat proteins to be in close proximity of the RNA replication area where there is a high concentration of viral RNAs (*67*).

The mechanism used by FHV for translating its nonpolyadenylated genomic RNAs is still unknown. There are different factors which must be initiated in order for translation to occur, and (+) ssRNA viruses seem to utilize an unknown approach when regulating their own translational machinery (*1*). Internal ribosome entry sites (IRES) have been shown to exist in many (+) ssRNA viruses; poliovirus was found to contain a region which promotes internal ribosome entry. The region located in the 5' untranslated regions of the RNA was

found to have many secondary and tertiary structures that promote the binding of the ribosomal subunit to the IRES start codon. IRES(s) have not been identified for FHV. The 3' untranslated region (UTR) found in positive stranded RNA viruses were found to contain structures which resemble tRNA-like elements (*68*). In eukaryotes translation is believed to occur in a closed loop formation with the 5' and 3' ends being brought close together. The key interaction is between the 3' poly A tail and the translation initiation factor 4E which binds the 5' cap (*68*). The effect of the poly A tail is to increase translational efficiency and provide stability to the RNA. The 3' UTR is thought to play a similar role in positive strand RNA viruses as the poly A tail; it was seen to enhance protein expression such as in the plant virus Alfalfa mosaic virus (AMV). The translational initiation factors used by FHV are not known, although it can be seen that coat protein translation is highly regulated and dependent on viral RNA replication.

3.5.2 RNA Replication

FHV forms a replication complex that is conserved among many (+)RNA virus families (*69*). RNA replication in FHV takes place on the outer mitochondrial membrane. Protein A, which is the Rd-RP, is the only protein required for replication. The N-terminus of protein A contains sequences for transport into the mitochondrial membrane and for insertion. Protein A acts as an integral membrane protein with the N-terminus inserted into the intermembrane space or the matrix and the C-terminus faces the cytoplasm. The movement of protein A to the mitochondrial membrane is independent of RNA replication. Electron microscopy revealed the formation approximately 50 nm membranous vesicles, located in the intermembrane space and bound to the outer mitochondrial membrane (Figure 5) (*70*). The FHV vesicle contains an opening of approximately 10 nm that allows for the flow of replication material to the cytoplasm (*70*). On average, each vesicle contains about 100 protein A molecules which associate with the mitochondrial membrane and with one another (*70, 71*). Protein A recruits RNA1 before RNA negative strand synthesis occurs, to

the mitochondrial membrane where the RNA replication complex will form (*47*). Recruitment of RNA1 to the replication site involves a cis-acting RNA element located between nt 68-205. In this region two stem loop structures exist, similar in sequence, and are essential for RNA1 recruitment (*72*). FHV uses cellular components to help form the replication complexes. It was demonstrated that by inhibiting the cell chaperone protein Hsp90 the synthesis of protein A was suppressed (*73*). The use of chaperone proteins to control distinct steps in viral RNA replication is found in other (+)RNA viruses, as are similarities in the formation of replication complexes.

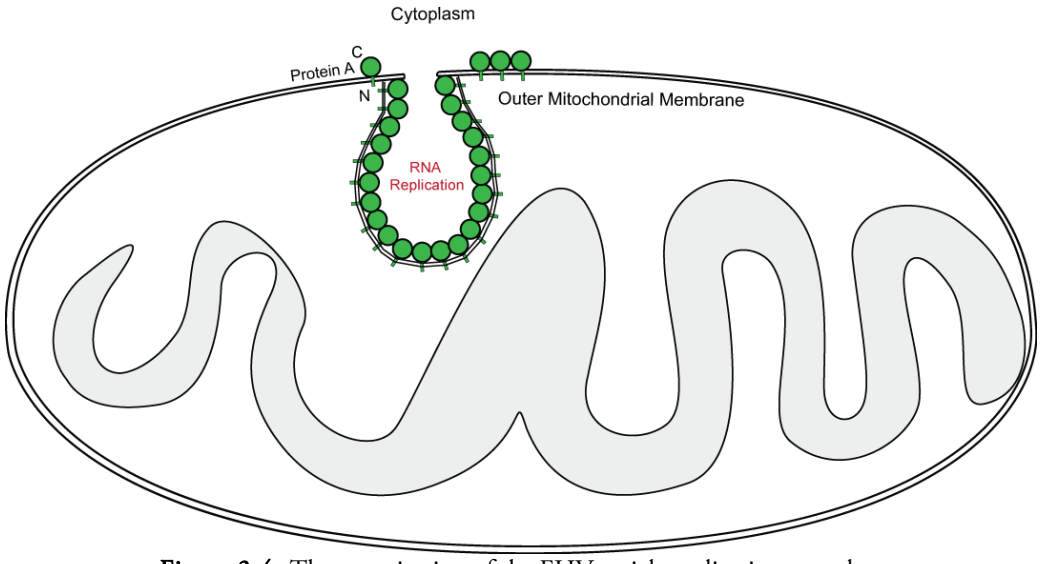

Figure 3.4- The organization of the FHV vesicle replication complex.
Protein A is represented by green circles showing the N-terminus being embedded in the membrane and the C-terminus exposed to the cytoplasm. A 10 nm opening connects the replication complex with the cytoplasm.

FHV displays a high degree of control in the replication of RNA1 and RNA2. Subgenomic RNA3 plays an important role in the replication process acting as a trans-activator for the replication of RNA2 (*74*). The exact mechanism of the transactivation has not been determined, but a signal involved has been located on the 3' end of RNA2 (*75*). The activation of RNA2 suppresses the transcription of RNA3 (*76*). It is believed that the regulation of RNA3 directs the replication of RNA1 and RNA2 (*74*). The mechanism used

by RNA1 to synthesize RNA3 has not been identified, although it is believed that premature termination is responsible for the synthesis of RNA3 (*77*). Premature termination is used by many plant viruses such as the Tomato bushy stunt virus and Red clover necrotic mosaic virus to regulate the subgenomic RNA expressions (*78*). Premature translation occurs with the synthesis of the negative sense RNA1 to end early, thereby creating the negative sense RNA3, which can then be use for the synthesis of the positive sense of RNA3 (*79*). A long distance base pairing interaction was observed in RNA1 that is required for RNA3 synthesis, similar to the interactions occurring in plant viruses; leading to the belief that long distance interaction in FHV may promote the synthesis of negative sense RNA1 to end early (*77, 78*). When RNA1 was supplied with a functional 5' replication element, the 108 nucleotide sequence at its 3' end was all that was required for its replication (*75*). The same sequence is found at the 3' end of the subgenomic RNA3 and may also act as replication element (*75*). Studies with RNA2 revealed that a minimum of 3 nucleotides are required at the 5' end for efficient replication (*80*). If the same 5' end requirements are needed for RNA1 replication, then RNA3 would contain the same 3 nucleotides required for replication (*79*). This concept was tested and was shown that RNA3 could be produced from RNA1 transcription and independent replication (*79*).

3.5.3 RNA Packaging

FHV exploits the plasticity of RNA to aid it in the packaging of the viral RNA genome. It was seen that packaged RNA takes on a dodecahedral structure within the virion. This is largely due to the plasticity of the RNA and its capability to form dynamic secondary structures (*81*). 10 bp regions located at each of the 2 fold axis appear visible in the X-ray structures. It is not known however which segments of the genome assume these positions. Through competition experiments it was observed that FHV preferably packages viral RNA over the cellular RNA. After the deletion of coat protein segments which recognize viral RNA, cellular RNA was packaged and adopted an indistinguishable dodecahedral structure

as the viral RNA (*81*). This also implies that it is not the RNA sequence which controls the organization inside the virion but the coat protein (*54, 81*). It was established that viral RNA does not fold spontaneously prior to packaging, since randomly packaged cellular RNA conforms to the same dodecahedron structure independent of its sequence and length. The possibility of packaging to occur during RNA replication has also been ruled out with pulse-chase experiments, showing that viral RNA is packaged with a 30 min delay (*82*). A likely explanation is that the capsid proteins act as chaperones as seen for the HIV nucleocapsid protein and the hepatitis delta virus antigen. The capsid proteins bind viral RNA stabilizing less favorable structures thereby facilitating proper assembly to occur (*54*).

FHV specific encapsidation sequences must be present on viral RNA and are used by capsid proteins to preferentially bind viral RNA with higher affinity than cellular RNA (*54*). Deletions and mutation studies on the C-terminus of FHV protein alpha, which becomes γ-peptide in the mature virion, showed complete loss of FHV genome recognition and resulted in the packaging of cellular RNA (*59*). The loss of viral RNA packaging was due to the deletion of the 44 residues of the C-terminus or single site amino acid substitutions of phenylalanines at positions 402, 405 and 407 (*59*). Deletion of residues 2-31 on the N-terminus of protein alpha yielded particles which differ in capsid structure and RNA content (*83*). The recognition of RNA2 was affected as the virions showed a decreased amount of RNA2 present inside (*83*). The region 35-49 of the N-terminus of the coat protein in FHV contains the arginine rich RNA binding motif (ARM) which is highly conserved among plant and non-plant viruses such as Brome mosaic virus and HIV (*84*). The substitution in the 32-50 region (ARM) of the N-terminus of all arginine residues to alanines resulted in the loss of RNA1 packaging specificity in FHV, and the viral particles contained only RNA2 (*85*). The highly positive nature of the ARM region is required for packaging, as was concluded with a substituted lysine mutant that retained packaging function. Fully functional viruses were also assembled when the ARM region of FHV was replaced by HIV-1 Rev protein, suggesting the importance of the region for recruiting viral RNA's to

replication sites. The recombinant baculovirus system showed that RNA1 was not required for virion assembly; when the cDNA of RNA2 was provided then the viral particles still formed mature FHV virions undistinguishable from authentic FHV virions (*86*).

Specific encapsidation sequences that promote the binding of the capsid protein to the viral RNA with high affinity as opposed to random cellular RNA have been identified for a number of viruses. The MS2 bacteriophage has a (+) ssRNA genome consisting of a single viral RNA. An RNA packaging signal sequence has been located on the MS2 phage, and it is a hairpin structure containing 19 nucleotides located at the 5' end of the replicase gene (*87, 88*). The coat protein dimer interacts with the hairpin loop and the unpaired adenine nucleotide in the hairpin (*89*). AMV packaging signal sequences have also been identified. The signal sequence is found at the 3'UTR in all AMV RNAs and is made up of 39 nucleotides (*90, 91*). The coat protein interacts with the AUGC repeats found at the bottom of the stem structures (*92*). The encapsidation sequences for viral RNAs are found at different positions throughout the genome and take on specific secondary structures which the capsid proteins can exploit and ensure viral RNA packaging during assembly.

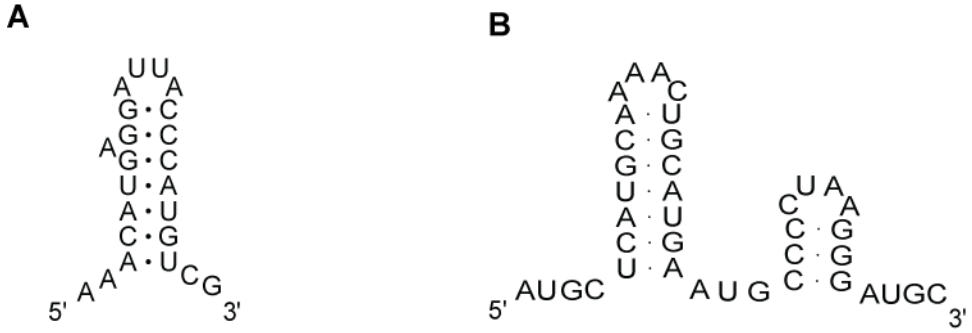

Figure 3.5- Capsid protein recognition sequences for viral RNAs of MS2 bacteriophage (**A**) and AMV (**B**).

Flock House virus has the smallest genome among RNA viruses (*44*). This feature and its wide host range make it an ideal choice for studying viral entry, replication and assembly. FHV being a (+) ssRNA icosahedral virus is part of a group of viruses to which many known

human pathogens belong to such as poliovirus, hepatitis A virus, human rhinoviruses, Norwalk group of viruses, and flaviviruses (*54*). Studying the mechanism of FHV assembly can aid in development of potential therapeutic agents which inhibit viral RNA packaging that can also be applied to other icosahedral (+) ssRNA viruses. The study of viral RNA packaging can also be applied to other RNA viruses (ex. influenza), as it is common among viruses to have many analogous mechanisms.

3.6 Research Objective

The capsid protein regions thought to interact with RNA1 and RNA2 during viral genome packaging have been identified by Dr. A. Schneemann. The N-terminal regions 1-31 and 32-50 of coat protein alpha are required for recognition of RNA2 and RNA1 respectively. The aim of this study is to identify the specific RNA and the sequence that interacts with the FHV coat protein (*59, 83*). The N-terminal regions identified as viral RNA packaging requirements will be used as targets to select for the RNA sequences with the dotLab system. The regions 1-30 and 31-58 from the N-terminus of protein alpha will construct the two selection targets. The full RNA1 and RNA2 sequences used in the binding selection can be obtained from NCBI gene bank under the accession numbers NC 004146 and NC 004144 respectively.

3.7 Materials and Methods

3.7.1 Minimization of RNase Contamination

A number of precautions were taken to minimize RNase contamination during RNA production. Fresh gloves were worn at all times. All preparation areas were wiped with RNase AWAY™. All buffers were made from nuclease-free Milli-Q water and autoclaved. All the labware used was wrapped in aluminum foil and autoclaved at 121 °C; prior to use it was washed with RNase AWAY™ followed by rinsing 3X with nuclease-free Milli-Q water. All plastic-ware utilized was RNase free certified by their respective manufacturers. During RNA synthesis reactions RNase inhibitor was added.

3.7.2 FHV Peptide

The FHV1 peptide containing one of the RNA selection target regions specifically amino acid residues 1-30 was ordered from Bachem. The peptide was ordered with a biotin moiety attached at the N-terminus and two additional alanine residues were added to provide a short linker region (Biotin-AAVNNNRPRRQRAQRVVVTTTQTAPVPQQNV).

3.7.3 Preparation of Plasmid DNA

Flock House virus RNA1 (3.1 kb) and RNA2 (1.4 kb) were each cloned into pSC-B vector (3.5 kb) and placed into Strataclone competent cells (Stratagene) by Dr. Elaine Collins. Cells containing plasmids pSC-B R1 and pSC-B R2 were grown on Luria-Bertani (LB) plates supplemented with ampicillin (100 µg/mL). A single isolated colony was selected from each LB plate and used to inoculate individual LB mediums containing ampicillin (100 µg/mL). 8 mL of the ampicillin-LB media were inoculated and incubated overnight at 37 °C. 5 mL of the overnight bacteria culture was processed for each plasmid. Further plasmid DNA

isolation and purification was done with the Wizard Plus SV Minipreps DNA purification system (Promega).

A 1% agarose gel containing 1.5 µL of ethidium bromide (10 mg/mL) was casted, to check if the plasmid DNA had been successfully purified. The gel was visualized by excitation at 365 nm with a 560 nm emission filter on the FluoroChem FC2 imaging illuminator coupled with AlphaEaseFC v.6.0 software (Alpha Innotech).

3.7.4 Linearization of Plasmid DNA

pSC-B R1 and pSC-B R2 were linearized with HindIII (Fermentas). Completed digestion of the plasmids was checked on 1% agarose gel containing 1.5 µL of ethidium bromide (10 mg/mL). Digestion reactions were cleaned up using QIAquick PCR purification kit (Qiagen). The concentration of the linearized plasmids was determined using the NanoDrop UV-Visible spectrophotometer (NanoDrop Technologies).

3.7.5 Synthesis of RNA

The transcription reaction mixture was setup as described in Table 3.1 for both pSC-B R1 and pSC-B R2 plasmids.

Table 3.1- Transcription reaction mixture.

Solution	Final Concentration
Tris-HCl buffer pH 7.5	80 mM
DTT	15 mM
$MgCl_2$	33 mM
Spermidine	1 mM
rATP, rGTP, rCTP, rUTP	3.75 mM each
Linearized template DNA	1 µg
RNase Inhibitor	1 unit/µL
T7 RNA polymerase	

The T7 RNA polymerase is added and the reaction is incubated at 37 °C for 4 hours. Once the transcription reaction is completed 1unit/ µL RQ DNase I (Promega) is added to the transcription reaction to destroy the DNA template. The reaction is incubated for an additional 15 minutes at 37 °C.

The transcription mixture was extracted with 1 volume of citrate-saturated phenol (pH 4.7):chloroform:isoamyl alcohol (125:24:1). The mixture was briefly vortexed and centrifuged at top speed in a tabletop Minispin microcentrifuge (Eppendorf). The upper aqueous layer is transferred to a new tube and extracted once more with 1 volume of chloroform:isoamyl alcohol (24:1). The top aqueous phase transferred to a new tube is ethanol precipitated with the addition of 1/10th the volume of sodium acetate (pH 5.2) and 2.5 volumes of cold 100% ethanol. The ethanol precipitation reaction is left at -80 °C for an hour or 10 minutes on dry ice; followed by centrifugation at maximum speed (4 °C). The pellet is washed with the total volume of the precipitation using cold 70% ethanol; followed by centrifugation at maximum speed (4 °C). The supernatant was removed and the remaining pellet is placed on dry ice for 10 min. and placed on the FreeZone Plus 4.5L console system lyophilizer (Labconco) to dry. The dried RNA is resuspended in nf. water.

3.7.6 Software

The RNA secondary structure figures were generated using mfold v.3.2 an RNA secondary structure prediction program, along with RnaViz v.2 software for producing RNA secondary structure drawings (*39-41*). Peptide sequences were made using ChemBioDraw Ultra 11.0 (CambridgeSoft). 3D protein modeling was done using UCSF Chimera v. 1.3 (*93*).

3.8 Results and Discussion

3.8.1 Plasmid DNA Isolation and Purification

After isolation and purification plasmids pSC-B R1 (6.6 kb) and pSC-B R2 (4.9 kb) were analyzed on a 1% agarose gel and visualized using ethidium bromide. Lambda DNA digested with EcoRI and HindIII was loaded onto the gel as a marker for size comparison. Figure 3.6 contains the agarose gel of the plasmids after purification. The gel indicates that the isolated and purified DNA plasmids are of the correct size (lane 1 and 2). The different size bands that appear for the two plasmids are due to the different conformations (relaxed, nicked, supercoiled) that the plasmid DNA can adopt.

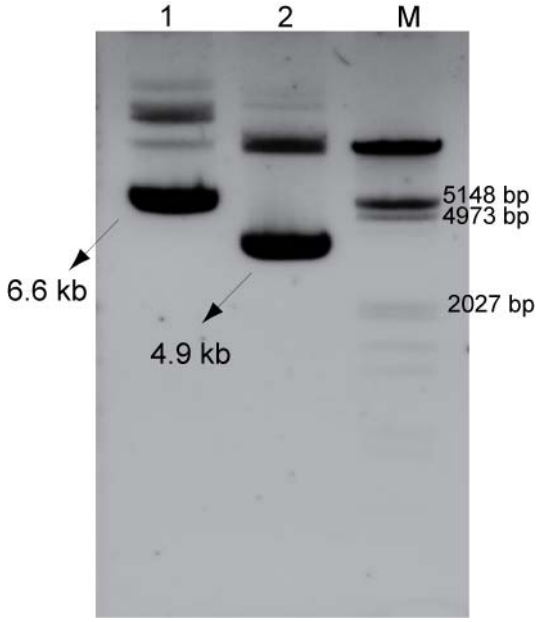

Figure 3.6- Agarose gel of plasmid DNA isolation and purification. pSC-B R1 and pSC-B R2 are shown in lanes 1 and 2 respectively. The lambda DNA/EcoRI + HindIII marker confirms the correct size plasmids have been isolated.

3.8.2 Linearization of Plasmid DNA

The linearization of pSC-B R1 and pSC-B R2 was done with the HindIII restriction endonuclease. Once the plasmids were fully digested, the removal of restriction enzyme was required for downstream purposes. The lambda/pUC mix marker was used for size determination of the linearized plasmids. The fully digested and purified plasmids containing RNA 1 and 2 inserts are observed on the agarose gel (Figure 3.7).

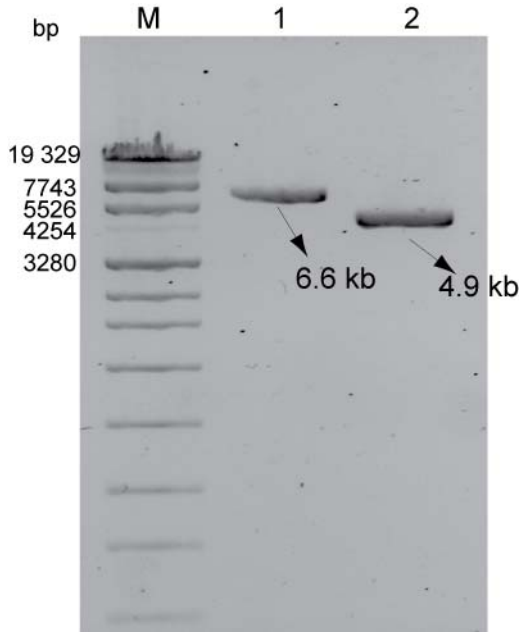

Figure 3.7- Purified linearized pSC-B R1 and pSC-B R2 plasmids.
Lane 1 and 2 show the completely linearized pSC-B R1 and pSC-B R2 plasmids of correct size, confirmed by the Lambda/pUC mix marker.

3.8.3 Gel Electrophoresis of In-vitro Transcriptions

The transcription reactions were assessed by electrophoresis on the Experion system to determine if the full length products of RNA 1 and RNA 2 have been synthesized. The virtual electrophoresis gel of the FHV RNA transcription reactions contains bands of incorrect size in addition to the correct transcript product (Figure 3.8). The correct size of 3.1 kb and 1.4 kb are present for FHV RNA 1 and RNA 2. There are several possibilities that may explain why shorter/longer transcript products are obtained along with the correct

full-length product. The first explanation to consider and easiest to confirm is that the size difference is caused by the Experion system. This may be due to an unknown interaction with fluorescent dye used to detect the RNA or with the components in the gel matrix. Using a different method to check the size of the RNA for instance a Formaldehyde or Glyoxal/DMSO agarose gel would determine if the problem lies with the Experion.

For fragments smaller in size it is known that they are not abortion products as they are too large in size. T7 polymerase produces abortion products early on in the transcription generating products ~6-10 nucleotides in length. These smaller abortion fragments will not be seen on the Experion system. It is possible that the transcription reaction conditions are not ideal for the home-made T7 enzyme causing the early removal of the enzyme from the template. Lowering the reaction temperature during transcription will slow down the T7 enzyme, and may prevent it from being displaced by any secondary structures in the template. The templates have been transcribed before in the lab by SP6 and T3 RNA polymerase and by other labs using the T7 RNA polymerase without any additional transcripts made. Therefore, it can be concluded that the problem is not sequence specific.

The presence of longer sized transcription products is more puzzling because in general longer templates have more stable transcription complexes and produce a larger amount of the desired RNA. It has been reported with shorter templates that abortion products complimentary at the 3' end to the RNA transcript can form RNA primed templates (*40*). These RNA primed templates can be extended by T7 to generate longer sized transcripts. With shorter templates the abortion products make up a larger percentage of the transcription yield increasing the probability for longer size RNA's. The correct size RNA may have to be gel purified on an agarose gel to remove the short/longer RNA's.

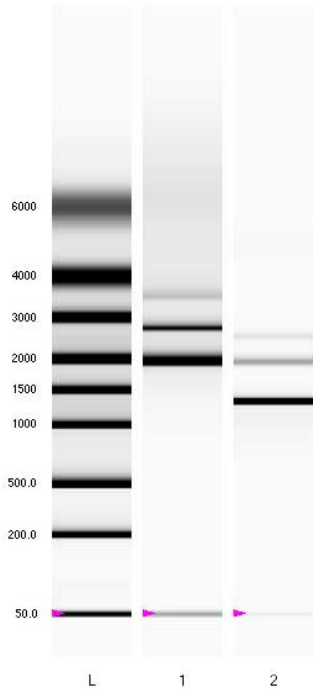

Figure 3.8- RNA electrophoresis virtual gel displaying transcription products from the transcribed linear pSC-B R1 and pSC-B R2 templates.

The arrow head indicates a 50bp fragment from the buffer used to standardize the sample with the RNA ladder (L). RNA 1 is shown in lane 1 and RNA 2 in lane 2, both transcriptions contain different length RNA's from the full-length product. Fluorescence spectra for each sample can be found in the appendices (Figure A1.2).

Chapter 4: Conclusions and Future Work

The aim of this study was to show the potential application of the dotLab system in characterizing RNA-protein interactions. The sensitivity of the system was tested with the well characterized Rev-RRE interaction from the HIV-1 virus. It was shown that the Rev peptide can be immobilized on the sensor surface via the avidin-biotin interaction, and the subsequent binding of the RRE could be detected on the dotLab system. The RNA-protein interaction was greatly affected by the immobilization techniques and steric hindrance at surface of the sensor.

Further research aimed at minimizing surface interactions possible with different biotin derivatives, in which a longer linker region is used to increase the height of the peptide and provide better access for the RRE RNA. Further work needs to be done to produce more consistent binding curves for the Rev-RRE interaction, from which kinetic data can be extracted and compared to existing kinetics for the Rev-RRE model. It would be interesting to perform preliminary binding studies with the Flock House virus using the dotLab system or a streptavidin paramagnetic bead pull-down assay. For this purpose production of sufficient amounts of full-length FHV RNA 1 and RNA 2 are required.

The results of this study indicate that the dotLab system is sensitive enough for the study of RNA-protein interactions and could be used for characterizing novel viral RNA binding sites used by viral proteins for viral RNA encapsidation.

REFERENCES

1. Flint, S. J. (2000) *Principles of virology : molecular biology, pathogenesis, and control*, ASM Press, Washington, D.C.

2. Forterre, P. (2006) The origin of viruses and their possible roles in major evolutionary transitions, *Virus Research 117*, 5-16.

3. Gesteland, R. F., Cech, T., and Atkins, J. F. (2006) *The RNA world : the nature of modern RNA suggests a prebiotic RNA*, 3rd ed., Cold Spring Harbor Laboratory Press, Cold Spring Harbor, NY.

4. Strauss, J. H., and Strauss, E. G. (1988) Evolution of RNA viruses, *Annual review of microbiology 42*, 657-683.

5. Domingo, E., and Holland, J. J. (1997) RNA virus mutations and fitness for survival, *Annual review of microbiology*, pp 151-178.

6. Schuck, P. (1997) Use of surface plasmon resonance to probe the equilibrium and dynamic aspects of interactions between biological macromolecules, *Annual Review of Biophysics and Biomolecular Structure*, pp 541-566.

7. (2007) Diffractive Optics Technology, *Technical Brief 101*, p 2, Axela Biosensors Inc., Toronto.

8. Tang, H., Kuhen, K. L., and Wong-Staal, F. (1999) Lentivirus replication and regulation, *Annual Review of Genetics*, pp 133-170.

9. Strauss, J. H., and Strauss, E. G. (2002) *Viruses and human disease*, Academic, San Diego, Calif. London.

10. Homann, S., Tibroni, N., Baumann, I., Sertel, S., Keppler, O. T., and Fackler, O. T. (2009) Determinants in HIV-1 Nef for enhancement of virus replication and depletion of CD4+ T lymphocytes in human lymphoid tissue ex vivo, *Retrovirology 6*.

11. Schwartz, O., Marechal, V., Danos, O., and Heard, J. M. (1995) Human immunodeficiency virus type 1 Nef increases the efficiency of reverse transcription in the infected cell, *Journal of virology 69*, 4053-4059.

12. Aiken, C., and Trono, D. (1995) Nef stimulates human immunodeficiency virus type 1 proviral DNA synthesis, *Journal of virology 69*, 5048-5056.

13. Heaphy, S., Dingwall, C., Ernberg, I., Gait, M. J., Green, S. M., Karn, J., Lowe, A. D., Singh, M., and Skinner, M. A. (1990) HIV-1 regulator of virion expression (Rev) protein binds to an RNA stem-loop structure located within the Rev response element region, *Cell 60*, 685-693.

14. Gorlich, D., and Kutay, U. (1999) Transport between the cell nucleus and the cytoplasm, *Annual review of cell and developmental biology*, pp 607-660.

15. Truant, R., and Cullen, B. R. (1999) The arginine-rich domains present in human immunodeficiency virus type 1 Tat and Rev function as direct importin β-dependent nuclear localization signals, *Molecular and Cellular Biology 19*, 1210-1217.

16. Henderson, B. R., and Percipalle, P. (1997) Interactions between HIV Rev and nuclear import and export factors: The Rev nuclear localisation signal mediates specific binding to human importin-β, *Journal of molecular biology 274*, 693-707.

17. Wen, W., Meinkoth, J. L., Tsien, R. Y., and Taylor, S. S. (1995) Identification of a signal for rapid export of proteins from the nucleus, *Cell 82*, 463-473.

18. Richard, N., Iacampo, S., and Cochrane, A. (1994) HIV-1 Rev is capable of shuttling between the nucleus and cytoplasm, *Virology 204*, 123-131.

19. Meyer, B. E., and Malim, M. H. (1994) The HIV-1 Rev trans-activator shuttles between the nucleus and the cytoplasm, *Genes and Development 8*, 1538-1547.

20. Tan, R., Chen, L., Buettner, J. A., Hudson, D., and Frankel, A. D. (1993) RNA recognition by an isolated alpha helix, *Cell 73*, 1031-1040.

21. Dillon, P. J., Nelblock, P., Perkins, A., and Rosen, C. A. (1990) Function of the human immunodeficiency virus types 1 and 2 Rev proteins is dependent on their ability to interact with a structured region present in env gene mRNA, *Journal of virology 64*, 4428-4437.

22. Kimura, T., and Ohyama, A. (1994) Interaction with the Rev response element along an extended stem I duplex structure is required to complete human immunodeficiency virus type 1 Rev-mediated trans-activation in vivo, *Journal of Biochemistry 115*, 945-952.

23. Mann, D. A., Mikaelian, I., Zemmel, R. W., Green, S. M., Lowe, A. D., Kimura, T., Singh, M., Butler, P. J. G., Gait, M. J., and Karn, J. (1994) A molecular rheostat. Co-operative Rev binding to stem I of the rev-response element modulates human immunodeficiency virus type-1 late gene expression, *Journal of molecular biology 241*, 193-207.

24. Peterson, R. D., Bartel, D. P., Szostak, J. W., Horvath, S. J., and Feigon, J. (1994) 1H NMR studies of the high-affinity Rev binding site of the Rev responsive element of HIV-1 mRNA: Base pairing in the core binding element, *Biochemistry 33*, 5357-5366.

25. Peterson, R. D., and Feigon, J. (1996) Structural change in Rev responsive element RNA of HIV-1 on binding Rev peptide, *Journal of molecular biology 264*, 863-877.

26. Battiste, J. L., Mao, H., Rao, N. S., Tan, R., Muhandiram, D. R., Kay, L. E., Frankel, A. D., and Williamson, J. R. (1996) α-Helix-RNA major groove recognition in an HIV-1 Rev peptide-RRE RNA complex, *Science 273*, 1547-1551.

27. Palmeri, D., and Malim, M. H. (1999) Importin β can mediate the nuclear import of an arginine-rich nuclear localization signal in the absence of importin α, *Molecular and Cellular Biology 19*, 1218-1225.

28. Adam, S. A., Marr, R. S., and Gerace, L. (1990) Nuclear protein import in permeabilized mammalian cells requires soluble cytoplasmic factors, *Journal of Cell Biology 111*, 807-816.

29. Pollard, V. W., and Malim, M. H. (1998) The HIV-1 Rev protein, *Annual review of microbiology*, pp 491-532.

30. Malim, M. H., and Cullen, B. R. (1991) HIV-1 structural gene expression requires the binding of multiple Rev monomers to the viral RRE: Implications for HIV-1 latency, *Cell 65*, 241-248.

31. Stade, K., Ford, C. S., Guthrie, C., and Weis, K. (1997) Exportin 1 (Crm1p) is an essential nuclear export factor, *Cell 90*, 1041-1050.

32. Fornerod, M., Ohno, M., Yoshida, M., and Mattaj, I. W. (1997) CRM1 is an export receptor for leucine-rich nuclear export signals, *Cell 90*, 1051-1060.

33. Fukuda, M., Asano, S., Nakamura, T., Adachi, M., Yoshida, M., Yanagida, M., and Nishida, E. (1997) CRM1 is responsible for intracellular transport mediated by the nuclear export signal, *Nature 390*, 308-311.

34. Ruhl, M., Himmelspach, M., Bahr, G. M., Hammerschmid, F., Jaksche, H., Wolff, B., Aschauer, H., Farrington, G. K., Probst, H., Bevec, D., and Hauber, J. (1993) Eukaryotic initiation factor 5A is a cellular target of the human immunodeficiency virus type 1 Rev activation domain mediating trans- activation, *Journal of Cell Biology 123*, 1309-1320.

35. Faijot, G., Sergeant, A., and Mikaelian, I. (1999) A new nucleoporin-like protein interacts with both HIV-1 Rev nuclear export signal and CRM-1, *Journal of Biological Chemistry 274*, 17309-17317.

36. Li, J., Tang, H., Mullen, T. M., Westberg, C., Reddy, T. R., Rose, D. W., and Wong-Staal, F. (1999) A role for RNA helicase A in post-transcriptional regulation of HIV type 1, *Proceedings of the National Academy of Sciences of the United States of America 96*, 709-714.

37. Pond, S. J. K., Ridgeway, W. K., Robertson, R., Wang, J., and Millar, D. P. (2009) HIV-1 Rev protein assembles on viral RNA one molecule at a time, *Proceedings of the National Academy of Sciences of the United States of America 106*, 1404-1408.

38. Wilkins, M. R., Gasteiger, E., Bairoch, A., Sanchez, J. C., Williams, K. L., Appel, R. D., and Hochstrasser, D. F. (1999) Protein identification and analysis tools in the ExPASy server, *Methods in molecular biology (Clifton, N.J.) 112*, 531-552.

39. De Rijk, P., Wuyts, J., and De Wachter, R. (2003) Rna Viz 2: An improved representation of RNA secondary structure, *Bioinformatics 19*, 299-300.

40. Nacheva, G. A., and Berzal-Herranz, A. (2003) Preventing nondesired RNA-primed RNA extension catalyzed by T7 RNA polymerase, *European Journal of Biochemistry 270*, 1458-1465.

41. Zuker, M. (2003) Mfold web server for nucleic acid folding and hybridization prediction, *Nucleic Acids Research 31*, 3406-3415.

42. Diamandis, E. P., and Christopoulos, T. K. (1991) The biotin-(strept)avidin system: Principles and applications in biotechnology, *Clinical Chemistry 37*, 625-636.

43. Scotti, P. D., Dearing, S., and Mossop, D. W. (1983) Flock House virus: a nodavirus isolated from Costelytra zealandica (White) (Coleoptera: Scarabaeidae), *Archives of virology 75*, 181-189.

44. Dasgupta, R., Free, H. M., Zietlow, S. L., Paskewitz, S. M., Aksoy, S., Shi, L., Fuchs, J., Hu, C., and Christensen, B. M. (2007) Replication of flock house virus in three genera of medically important insects, *Journal of medical entomology 44*, 102-110.

45. Dasmahapatra, B., Dasgupta, R., Ghosh, A., and Kaesberg, P. (1985) Structure of the black beetle virus genome and its functional implications, *Journal of molecular biology 182*, 183-189.

46. Ball, L. A. (1997) Nodavirus RNA recombination, *Seminars in Virology 8*, 95-100.

47. Van Wynsberghe, P. M., Chen, H. R., and Ahlquist, P. (2007) Nodavirus RNA replication protein A induces membrane association of genomic RNA, *Journal of virology 81*, 4633-4644.

48. Chao, J. A., June, H. L., Chapados, B. R., Debler, E. W., Schneemann, A., and Williamson, J. R. (2005) Dual modes of RNA-silencing suppression by Flock House virus protein B2, *Nature Structural and Molecular Biology 12*, 952-957.

49. Schneemann, A., Zhong, W., Gallagher, T. M., and Rueckert, R. R. (1992) Maturation cleavage required for infectivity of a nodavirus, *Journal of virology 66*, 6728-6734.

50. Zlotnick, A., Reddy, V. S., Dasgupta, R., Schneemann, A., Ray Jr, W. J., Rueckert, R. R., and Johnson, J. E. (1994) Capsid assembly in a family of animal viruses primes an autoproteolytic maturation that depends on a single aspartic acid residue, *Journal of Biological Chemistry 269*, 13680-13684.

51. Rossmann, M. G., and Johnson, J. E. (1989) Icosahedral RNA virus structure, *Annual Review of Biochemistry 58*, 533-573.

52. Cheng, R. H., Reddy, V. S., Olson, N. H., Fisher, A. J., Baker, T. S., and Johnson, J. E. (1994) Functional implications of quasi-equivalence in a T = 3 icosahedral animal virus established by cryo-electron microscopy and X-ray crystallography, *Structure 2*, 271-282.

53. Fisher, A. J., and Johnson, J. E. (1993) Ordered duplex RNA controls capsid architecture in an icosahedral animal virus, *Nature 361*, 176-179.

54. Schneemann, A. (2006) The structural and functional role of RNA in icosahedral virus assembly, *Annual review of microbiology 60*, 51-67.

55. Tsai, B. (2007) Penetration of nonenveloped viruses into the cytoplasm, *Annual review of cell and developmental biology 23*, 23-43.

56. Hogle, J. M. (2002) Poliovirus cell entry: common structural themes in viral cell entry pathways, *Annual review of microbiology 56*, 677-702.

57. Bothner, B., Dong, X. F., Bibbs, L., Johnson, J. E., and Siuzdak, G. (1998) Evidence of viral capsid dynamics using limited proteolysis and mass spectrometry, *The Journal of biological chemistry 273*, 673-676.

58. Walukiewicz, H. E., Johnson, J. E., and Schneemann, A. (2006) Morphological changes in the T=3 capsid of flock house virus during cell entry, *Journal of virology 80*, 615-622.

59. Schneemann, A., and Marshall, D. (1998) Specific encapsidation of nodavirus RNAs is mediated through the C terminus of capsid precursor protein alpha, *Journal of virology 72*, 8738-8746.

60. Bong, D. T., Janshoff, A., Steinem, C., and Ghadiri, M. R. (2000) Membrane partitioning of the cleavage peptide in flock house virus, *Biophysical journal 78*, 839-845.

61. Bong, D. T., Steinem, C., Janshoff, A., Johnson, J. E., and Ghadiri, M. R. (1999) A highly membrane-active peptide in Flock House virus: Implications for the mechanism of nodavirus infection, *Chemistry and Biology 6*, 473-481.

62. Janshoff, A., Bong, D. T., Steinem, C., Johnson, J. E., and Ghadiri, M. R. (1999) An animal virus-derived peptide switches membrane morphology: Possible relevance to nodaviral transfection processes, *Biochemistry 38*, 5328-5336.

63. Maia, L. F., Soares, M. R., Valente, A. P., Almeida, F. C. L., Oliveira, A. C., Gomes, A. M. O., Freitas, M. S., Schneemann, A., Johnson, J. E., and Silva, J. L. (2006) Structure of a membrane-binding domain from a non-enveloped animal virus:

Insights into the mechanism of membrane permeability and cellular entry, *Journal of Biological Chemistry 281*, 29278-29286.

64. Galiana-Arnoux, D., Dostert, C., Schneemann, A., Hoffmann, J. A., and Imler, J. L. (2006) Essential function in vivo for Dicer-2 in host defense against RNA viruses in drosophila, *Nature Immunology 7*, 590-597.

65. Ortin, J., and Parra, F. (2006) Structure and function of RNA replication, *Annual review of microbiology 60*, 305-326.

66. Venter, P. A., and Schneemann, A. (2007) Assembly of two independent populations of flock house virus particles with distinct RNA packaging characteristics in the same cell, *Journal of virology 81*, 613-619.

67. Venter, P. A., Krishna, N. K., and Schneemann, A. (2005) Capsid protein synthesis from replicating RNA directs specific packaging of the genome of a multipartite positive-strand RNA virus, *Journal of virology 79*, 6239-6248.

68. Dreher, T. W., and Miller, W. A. (2006) Translational control in positive strand RNA plant viruses, *Virology 344*, 185-197.

69. Miller, D. J., Schwartz, M. D., and Ahlquist, P. (2001) Flock house virus RNA replicates on outer mitochondrial membranes in Drosophila cells, *Journal of virology 75*, 11664-11676.

70. Kopek, B. G., Perkins, G., Miller, D. J., Ellisman, M. H., and Ahlquist, P. (2007) Three-dimensional analysis of a viral RNA replication complex reveals a virus-induced mini-organelle, *PLoS Biology 5*, 2022-2034.

71. Dye, B. T., Miller, D. J., and Ahlquist, P. (2005) In vivo self-interaction of nodavirus RNA replicase protein a revealed by fluorescence resonance energy transfer, *Journal of virology 79*, 8909-8919.

72. Van Wynsberghe, P. M., and Ahlquist, P. (2009) 5' cis elements direct nodavirus RNA1 recruitment to mitochondrial sites of replication complex formation, *Journal of virology 83*, 2976-2988.

73. Castorena, K. M., Weeks, S. A., Stapleford, K. A., Cadwallader, A. M., and Miller, D. J. (2007) A functional heat shock protein 90 chaperone is essential for efficient

flock house virus RNA polymerase synthesis in Drosophila cells, *Journal of virology 81*, 8412-8420.

74. Eckerle, L. D., and Ball, L. A. (2002) Replication of the RNA segments of a bipartite viral genome is coordinated by a transactivating subgenomic RNA, *Virology 296*, 165-176.

75. Albarino, C. G., Eckerle, L. D., and Ball, L. A. (2003) The cis-acting replication signal at the 3' end of Flock House virus RNA2 is RNA3-dependent, *Virology 311*, 181-191.

76. Zhong, W., and Rueckert, R. R. (1993) Flock house virus: down-regulation of subgenomic RNA3 synthesis does not involve coat protein and is targeted to synthesis of its positive strand, *Journal of virology 67*, 2716-2722.

77. Lindenbach, B. D., Sgro, J. Y., and Ahlquist, P. (2002) Long-distance base pairing in flock house virus RNA1 regulates subgenomic RNA3 synthesis and RNA2 replication, *Journal of virology 76*, 3905-3919.

78. Miller, W. A., and White, K. A. (2006) Long-distance RNA-RNA interactions in plant virus gene expression and replication, *Annual review of phytopathology 44*, 447-467.

79. Eckerle, L. D., Albarino, C. G., and Ball, L. A. (2003) Flock House virus subgenomic RNA3 is replicated and its replication correlates with transactivation of RNA2, *Virology 317*, 95-108.

80. Ball, L. A. (1994) Replication of the genomic RNA of a positive-strand RNA animal virus from negative-sense transcripts, *Proceedings of the National Academy of Sciences of the United States of America 91*, 12443-12447.

81. Tihova, M., Dryden, K. A., Le, T. V., Harvey, S. C., Johnson, J. E., Yeager, M., and Schneemann, A. (2004) Nodavirus coat protein imposes dodecahedral RNA structure independent of nucleotide sequence and length, *Journal of virology 78*, 2897-2905.

82. Gallagher, T. M., and Rueckert, R. R. (1988) Assembly-dependent maturation cleavage in provirions of a small icosahedral insect ribovirus, *Journal of virology 62*, 3399-3406.

83. Marshall, D., and Schneemann, A. (2001) Specific packaging of nodaviral RNA2 requires the N-terminus of the capsid protein, *Virology 285*, 165-175.

84. Rao, A. L. (2006) Genome packaging by spherical plant RNA viruses, *Annual review of phytopathology 44*, 61-87.

85. Venter, P. A., Marshall, D., and Schneemann, A. (2009) Dual roles for an arginine-rich motif in specific genome recognition and localization of viral coat protein to RNA replication sites in flock house virus-infected cells, *Journal of virology 83*, 2872-2882.

86. Schneemann, A., Dasgupta, R., Johnson, J. E., and Rueckert, R. R. (1993) Use of recombinant baculoviruses in synthesis of morphologically distinct viruslike particles of flock house virus, a nodavirus, *Journal of virology 67*, 2756-2763.

87. Johansson, H. E., Dertinger, D., Lecuyer, K. A., Behlen, L. S., Greef, C. H., and Uhlenbeck, U. C. (1998) A thermodynamic analysis of the sequence-specific binding of RNA by bacteriophage MS2 coat protein, *Proceedings of the National Academy of Sciences of the United States of America 95*, 9244-9249.

88. Stockley, P. G., Stonehouse, N. J., Murray, J. B., Goodman, S. T., Talbot, S. J., Adams, C. J., Liljas, L., and Valegard, K. (1995) Probing sequence-specific RNA recognition by the bacteriophage MS2 coat protein, *Nucleic Acids Res 23*, 2512-2518.

89. Valegard, K., Murray, J. B., Stonehouse, N. J., Van Den Worm, S., Stockley, P. G., and Liljas, L. (1997) The three-dimensional structures of two complexes between recombinant MS2 capsids and RNA operator fragments reveal sequence-specific protein-RNA interactions, *Journal of molecular biology 270*, 724-738.

90. Reusken, C. B. E. M., and Bol, J. F. (1996) Structural elements of the 3'-terminal coat protein binding site in alfalfa mosaic virus RNAs, *Nucleic Acids Research 24*, 2660-2665.

91. Laforest, S. M., and Gehrke, L. (2004) Spatial determinants of the alfalfa mosaic virus coat protein binding site, *RNA (New York, N.Y) 10*, 48-58.

92. Houser-Scott, F., Baer, M. L., Liem Jr, K. F., Cai, J. M., and Gehrke, L. (1994) Nucleotide sequence and structural determinants of specific binding of coat protein or coat protein peptides to the 3' untranslated region of alfalfa mosaic virus RNA 4, *Journal of virology 68*, 2194-2205.

93. Pettersen, E. F., Goddard, T. D., Huang, C. C., Couch, G. S., Greenblatt, D. M., Meng, E. C., and Ferrin, T. E. (2004) UCSF Chimera - A visualization system for exploratory research and analysis, *Journal of Computational Chemistry 25*, 1605-1612.

94. Selo, I., Negroni, L., Creminon, C., Grassi, J., and Wal, J. M. (1996) Preferential labeling of alpha-amino N-terminal groups in peptides by biotin: Application to the detection of specific anti-peptide antibodies by enzyme immunoassays, *Journal of Immunological Methods 199*, 127-138.

APPENDICES

A1. Supplementary Information

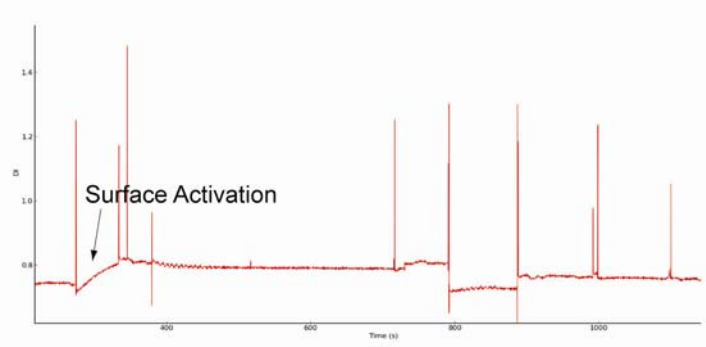

Figure A1.1- Amine sensor surface activation with failed Bt-Rev coupling and RRE binding.

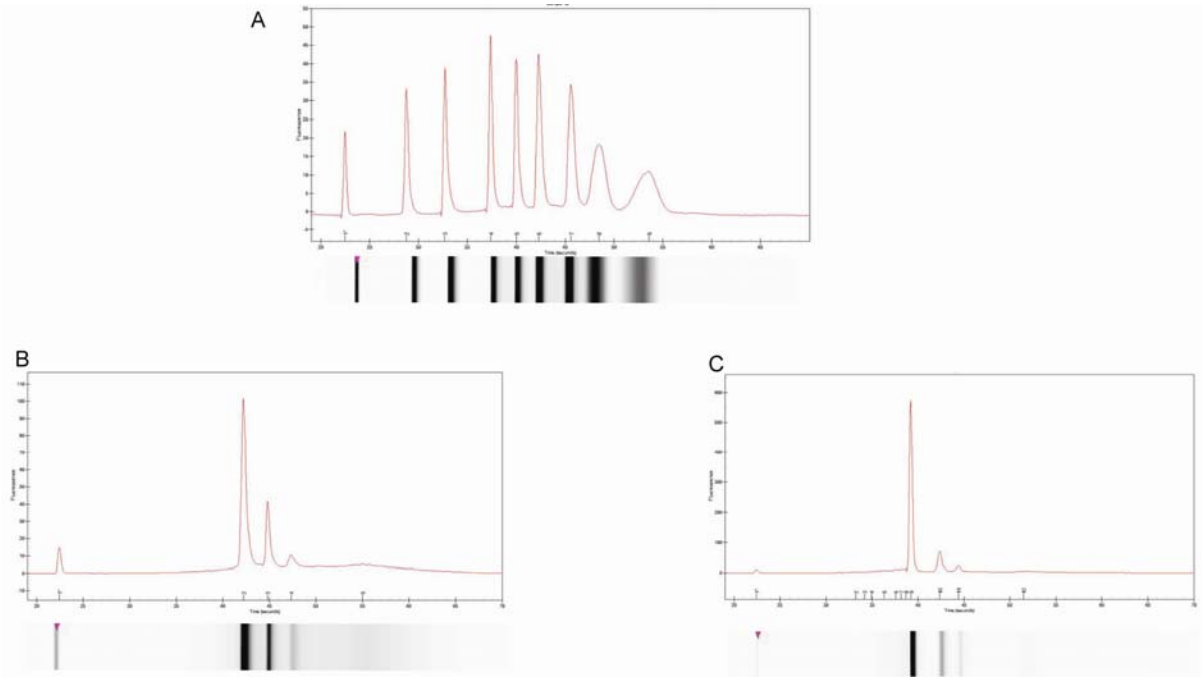

Figure A1.2- Fluorescence spectra intensities used to compose virtual gel images.
The virtual gel images are aligned with their respective spectra and peaks.

A2. Labeling and Purification of eNOS peptide

The dotLab system was to be used to study the binding interaction between eNOS and Cam. The 20 residue eNOS peptide (TRKKTFKEVANAVKISASLM) was to be monitored binding to Cam on an amine sensor.

The coupling of Cam (16.7 kDa) protein to the amine sensor surface was unsuccessful with no change in the diffractive index. Prior to coupling Cam to the sensor buffer exchange had to be performed in order to remove the amine containing buffer (Tris). The coupling of the eNOS peptide to the amine sensor was attempted and no surface coupling could be detected. Some of the reasons that could have contributed to no detection of binding are:

- The coupling reactions of Cam may have had trace amounts of free amines in the buffer that were not sufficiently removed by buffer exchange, thereby preventing coupling to the surface.
- The eNOS peptide and Cam possibly did not produce a large enough change in the sensor surface upon coupling for detection.
- Immobilization effecting the conformation of the coupled molecules and steric hindrance from nearby molecules could have impacted binding.

It should be possible to see the coupling of either eNOS peptide or Cam to the sensor surface, since surface activation alone is enough to produce a detectable change. Reducing protein concentrations and incubation periods could enhance coupling and subsequent binding steps. Exploring other coupling chemistries that could be performed on the sensors without damaging effects by modifying the carboxyl groups could provide more effective means and enhance coupling reactions.

It was decided that the avidin sensors may be a better initial approach because the biotin moiety would provide increased length from the sensor surface. The use of the avidin sensor would require N-terminally biotin labeled eNOS peptide. The biotinylation reaction was carried out in the same manner as for the Rev peptide. More caution had to be taken with

labeling eNOS due to the presence of 4 lysine residues that could be labeled as well besides the N-terminal amine. The buffer used for labeling was at pH 6.5; this promotes labeling of the N-terminal amine group. The biotinylation reaction occurs with primary amines that are not in their protonated form. At pH 6.5 the amount of protonated amines will be higher for lysine side chain amine groups (pKa 10.5) than the N-terminal amines (pKa 9.0). The ratio of non-protonated amines will be higher for the N-terminal amines thus promoting labeling at the N-terminus. eNOS can be labeled in different amounts, with only one binding site labeled to all the binding sites labeled (Table A2.1).

Table A2.1- Possible eNOS modifications with biotin labeling.

# of Biotin Labels	Mass of eNOS (Da)
0	2223
1	2448
2	2675
3	2901
4	3127
5	3354

The labeling reaction and purification for eNOS were performed as previously described for Rev in Section 2.5.5 Labeling and Purification of Rev Peptide. The elution profile of labeled eNOS shows 12 separate peaks (Figure A2.1). The numbered peaks were characterized by positive ion mode mass spectrometry. Only early eluted peaks were identified because the N-terminally labeled peptide should elute at the beginning as was indicated by Selo, I. *et al (94)*.

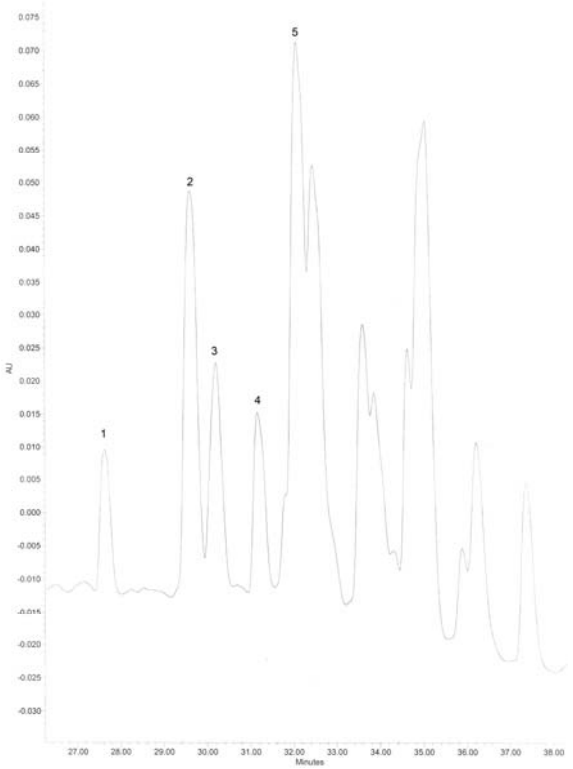

Figure A2.1- Elution profile of the 2 hour biotinylation reaction of eNOS. The peaks that were further characterized are numbered from 1-5.

Mass spectrometry characterization of the individual fractions (Figures A2.2-A2.6) indicated that the N-terminally labeled protein could be in either 2nd or 3rd fraction. The single biotin labeled peptide could be the biotin located at the N-terminal or at any of the lysine residues in the peptide. The labeled peptide could be used on the biotin sensor to check if Cam still binds or digestion with a specific protease. Cleavage products could then be used to determine at which position the peptide is labeled.

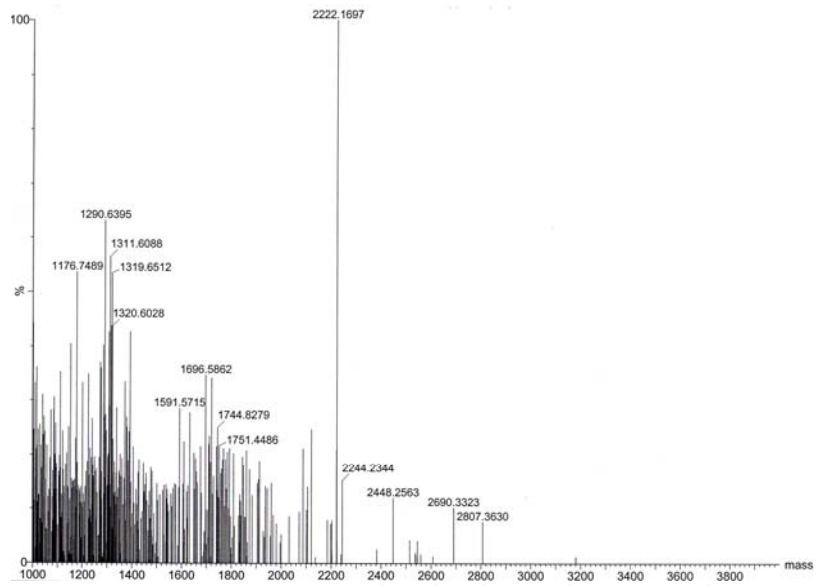

Figure A2.2- Mass spectrum characterization of the first fraction from the purification elution profile. The major peak indicates the fraction contains unlabeled eNOS peptide.

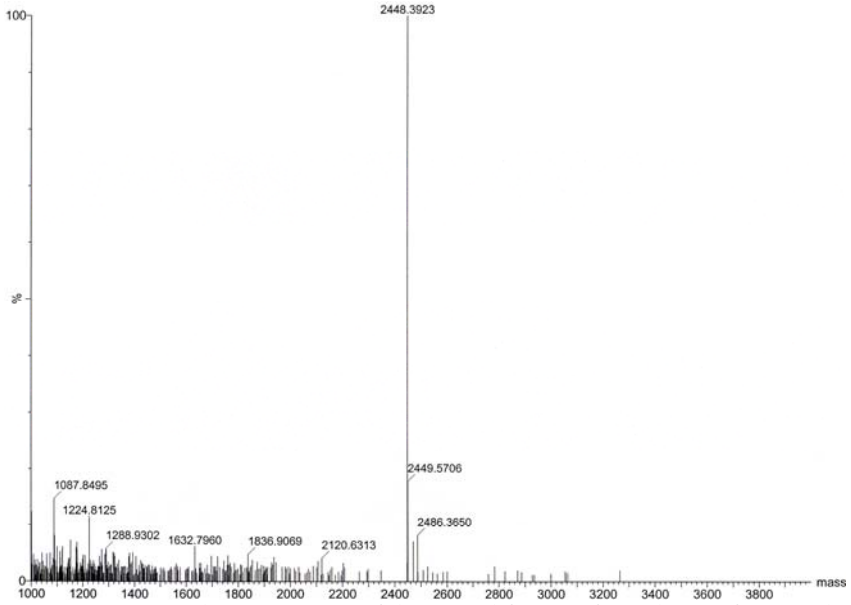

Figure A2.3- Mass spectrum characterization of the second fraction from the purification elution profile. The major peak indicates the fraction contains eNOS peptide with a single biotin label.

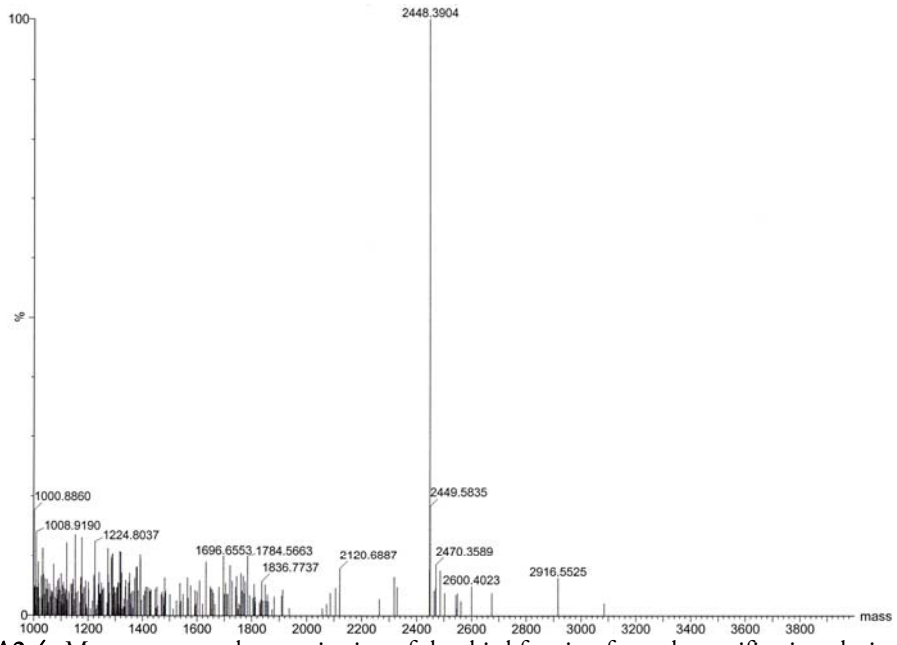

Figure A2.4- Mass spectrum characterization of the third fraction from the purification elution profile. The major peak indicates the fraction also contains eNOS with a single biotin label.

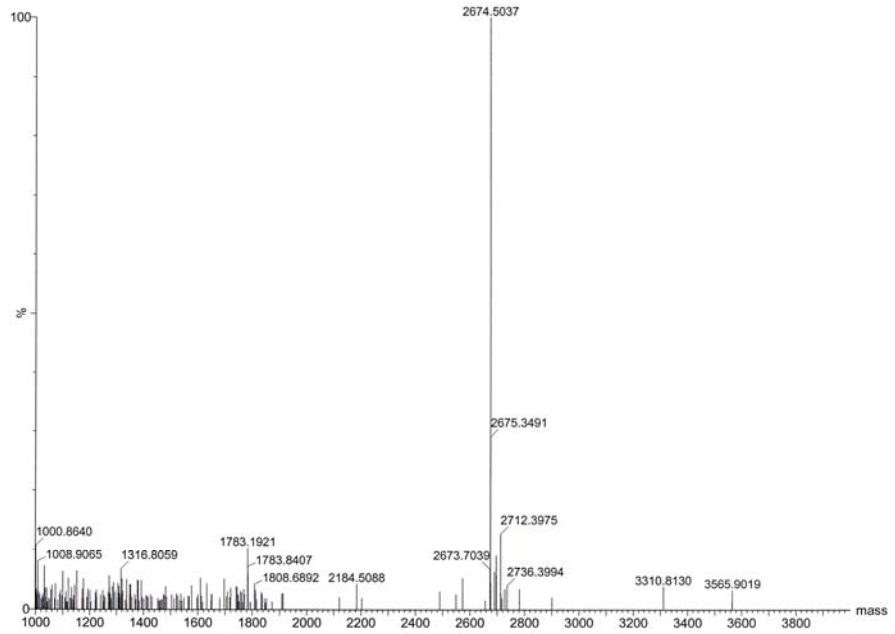

Figure A2.5- Mass spectrum characterization of the fourth fraction from the purification elution profile. The major peak indicates the fraction contains eNOS with two biotin labels.

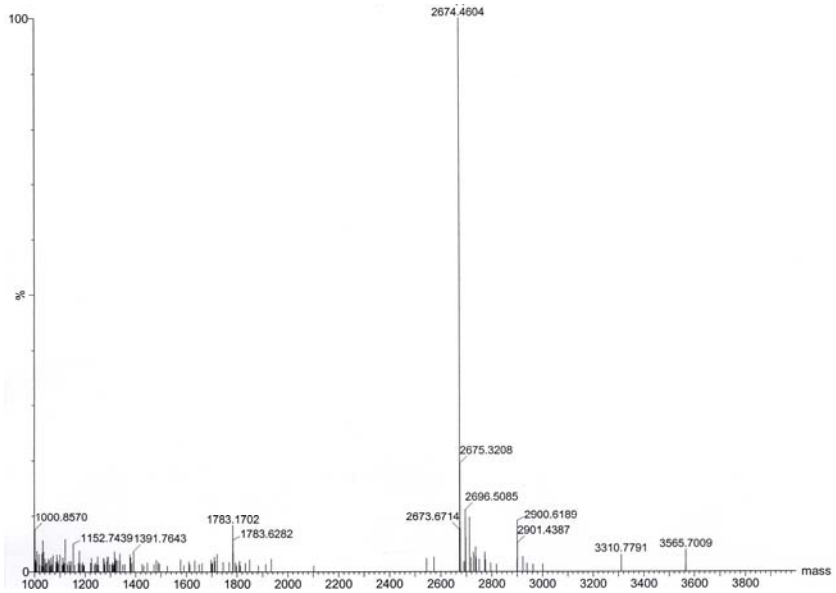

Figure A2.6- Mass spectrum characterization of the fifth fraction from the purification elution profile**.** The major peak indicates the fraction contains eNOS with two biotin labels and a trace of peptide containing three biotin labels.